Human Molecular Genetics, 2016, Vol. 25, No. 14 3011–3028

doi: 10.1093/hmg/ddw155
Advance Access Publication Date: 23 June 2016
Original Article

ORIGINAL ARTICLE

Cilia gene mutations cause atrioventricular septal defects by multiple mechanisms

Ozanna Burnicka-Turek[1,†,*], Jeffrey D. Steimle[1], Wenhui Huang[2], Lindsay Felker[2], Anna Kamp[1], Junghun Kweon[1], Michael Peterson[1], Roger H. Reeves[3], Cheryl L. Maslen[4], Peter J. Gruber[5], Xinan H. Yang[1], Jay Shendure[2] and Ivan P. Moskowitz[1,†,*]

[1]Departments of Pediatrics, Pathology, and Human Genetics, The University of Chicago, Chicago, IL 60637, USA, [2]Department of Genome Sciences, University of Washington, Seattle, WA 98195, USA, [3]Department of Physiology and Institute for Genetic Medicine, Johns Hopkins University School of Medicine, Baltimore, MD 21205, USA, [4]Knight Cardiovascular Institute and Department of Molecular and Medical Genetics, Oregon Health & Science University, Portland, OR 97239, USA and [5]Department of Cardiothoracic Surgery, University of Iowa, Iowa City, IA 52245, USA

*To whom the correspondence should be addressed at: Departments of Pediatrics, Pathology, and Human Genetics, The University of Chicago, 900 East 57th Street, KCBD Room 5102, Chicago, IL 60637, USA. Tel: 773/834-0462; Fax: 773/834-2132; Email: imoskowitz@uchicago.edu (I.P.M.), Email: burnickatureko@uchicago.edu (O.B.T.).

Abstract

Atrioventricular septal defects (AVSDs) are a common severe form of congenital heart disease (CHD). In this study we identified deleterious non-synonymous mutations in two cilia genes, *Dnah11* and *Mks1*, in independent N-ethyl-N-nitrosourea-induced mouse mutant lines with heritable recessive AVSDs by whole-exome sequencing. Cilia are required for left/right body axis determination and second heart field (SHF) Hedgehog (Hh) signaling, and we find that cilia mutations affect these requirements differentially. *Dnah11*^{avc4} did not disrupt SHF Hh signaling and caused AVSDs only concurrently with heterotaxy, a left/right axis abnormality. In contrast, *Mks1*^{avc6} disrupted SHF Hh signaling and caused AVSDs without heterotaxy. We performed unbiased whole-genome SHF transcriptional profiling and found that cilia motility genes were not expressed in the SHF whereas cilia structural and signaling genes were highly expressed. SHF cilia gene expression predicted the phenotypic concordance between AVSDs and heterotaxy in mice and humans with cilia gene mutations. A two-step model of cilia action accurately predicted the AVSD/heterotaxyu phenotypic expression pattern caused by cilia gene mutations. We speculate that cilia gene mutations contribute to both syndromic and non-syndromic AVSDs in humans and provide a model that predicts the phenotypic consequences of specific cilia gene mutations.

Introduction

Congenital heart disease (CHD), or structural heart defects present at birth, is the most common birth defect associated with significant morbidity and mortality worldwide (1–3), yet most of the genetic contribution to CHD remains undescribed (1). Atrioventricular septal defects (AVSDs [MIM: 606215]) are a class of CHD with septal defects at or adjacent to the level of the AV valves, including atrial septal defects of the primum type,

†O.B.T and I.P.M. are co-corresponding authors.
Received: December 2, 2015. **Revised:** May 13, 2016. **Accepted:** May 18, 2016

© The Author 2016. Published by Oxford University Press.
All rights reserved. For permissions, please e-mail: journals.permissions@oup.com

ventricular septal defects of the inflow type, or complete common AV canal spanning the atria and ventricles. AVSDs comprise 5–10% of CHD and a greater proportion of cases with significant morbidity and mortality (4). Patients with AVSDs have a higher recurrence rate of CHD among their offspring compared with patients with other types of CHD (5). In familial non-syndromic CHD, the phenotypic concurrence for AVSD between affected family members is much higher than that for most other types of CHD (6,7). We previously performed a forward genetic screen in mice that demonstrated more uniform expressivity of familial AVSDs than other forms of CHD (8). These observations suggested that AVSDs might have a tractable genetic basis. We identified and propagated six murine lines with heritable recessive AVSDs (8).

The paradigm for the developmental basis of AVSDs has undergone recent revision. AVSDs were historically attributed to defects in endocardial cushion development within the heart (4). However, recent work supports a paradigm for the developmental basis of AVSDs based on defects in second heart field (SHF) cardiac progenitors (9–12). The entire atrial septum derives from the SHF and molecular events in the SHF are required for AV septation (11–15). Furthermore, morphologic analysis of AVSDs in human embryos has revealed a specific deficiency of the SHF-derived dorsal mesenchymal protrusion (DMP) (also known as the spina vestibuli or vestibular spine) (16). These observations suggest that the developmental basis of AVSDs results at least in part from deficiency of the SHF-derived DMP (17).

AV septation and DMP development require cilia-based Hedgehog (Hh) signaling (12,13), the requirement of the primary cilium for Hh signaling is well-established (18,19), and cilia are structurally present in the SHF (20). Observations consistent with a role for cilia-based Hh signaling in AV septation include: (i) SHF-specific deletion of Hh signaling genes causes AVSDs (13); (ii) The atrial septum is composed of a lineage derived from Hh-receiving SHF cardiac progenitors (12); (iii) cilia function is required for SHF Hh signaling and AV septation (18); and (iv) Hh signaling and cardiogenic transcription factors collaborate in AV septation [11]. These observations suggest that cilia and Hh signaling components may contribute to the genetic basis of human AVSDs. Consistent with this hypothesis, the first human gene implicated in simplex AVSD (AVSD that present as singular defects without other organ system (syndromic) manifestations), *CRELD1* (MIM: 607170) (21) has been identified as a component of cilia (http://www.sfu.ca/~leroux/ciliome_database.htm) (22).

Cilia are also required for the establishment of embryonic L/R patterning (23). Cilia gene mutations are a cause of laterality defects, termed heterotaxy syndrome or situs ambiguous (23). Heterotaxy syndrome is characterized by randomization of the left/right body plan axis, affecting the morphogenesis of visceral organs that normally display laterality, including the heart. AVSDs and heterotaxy syndrome are strongly associated: AVSDs are the most common form of CHD in heterotaxy syndrome and approximately two-third of heterotaxy cases demonstrate AVSDs (23–28). Furthermore, a significant fraction of AVSD cases are observed in the background of heterotaxy. The degree of concurrence between heterotaxy syndrome and AVSD supports a potential common etiology (23–28). Moreover, the requirement for cilia function in both L/R determination and for AV-septum progenitor cells specification suggests that cilia function may provide a mechanistic link underlying the co-occurrence of AVSDs and heterotaxy syndrome.

In this study, we defined the genetic causation of AVSDs in two independent mouse lines, *avc4* and *avc6*, by whole exome sequencing (WES). Line *avc4* harbored a recessive mutant allele of dynein, axonemal heavy chain 11 (*Dnah11*) and *avc6* a recessive mutant allele of Meckel syndrome, type 1 (*Mks1*). $Dnah11^{avc4}$ homozygous mutant mice harbored AVSDs in a minority of cases and only when situs abnormalities were observed. *Dnah11* expression was absent from the wild-type embryonic SHF and heart, and $Dnah11^{avc4}$ mutant mice demonstrated normal SHF Hh signaling. In contrast, $Mks1^{avc6}$ homozygous mutant mice always showed AVSDs, although situs abnormalities were infrequent. *Mks1* was strongly expressed in the murine SHF and $Mks1^{avc6}$ embryos showed a significant SHF Hh signaling decrement. The literature revealed AVSDs associated with mutations in 22 mouse and 7 human cilia genes (Tables 2 and 3). AVSD/situs concordance for *Dnah11* mutants matched that reported for cilia motility gene mutations whereas AVSD/situs concordance for *Mks1* mutants matched that reported for cilia structural/signaling gene mutations. We performed unbiased transcriptome analysis of the murine SHF by RNA-seq and showed that cilia motility genes were not expressed whereas the cilia structural and signaling genes were highly expressed. A model based on a requirement for cilia function in two separable roles, L/R determination and SHF Hh signaling, defines three classes of cilia gene mutations and accurately predicts the distinct expressivity of AVSDs and heterotaxy observed in mice and humans with cilia mutations.

Results

WES of mouse lines AV canal 2–6 (*avc2–6*)

We previously conducted a forward genetic screen and mapped N-ethyl-N-nitrosourea (ENU)-induced mutations causing AVSDs in six lines, atrioventricular canal 1–6 (*avc1–6*), to distinct loci on five mouse chromosomes (Table 1) (8,18). *Avc1* was previously identified as a mutant allele of intraflagellar transport protein 172 ($Ift172^{avc1}$), a gene required for cilia biogenesis and Hh signaling (Table 1) (18,19). Mutation recovery in the remaining five *avc* lines (*avc2–6*) was conducted using WES analysis. We applied a filtering strategy that only retained variants that were homozygous in the affected mouse, that were absent from other strains exome-sequenced for this or other unrelated projects (15 comparator strains in total), and that were located within the mapped interval for each line, respectively. Single homozygous coding mutations were identified in *avc4* and *avc6* (Table 1). No homozygous coding or splice site variants were identified in lines *avc3* and *avc5* (Table 1). Multiple coding variants were found in the *avc2* line and identification of the causative mutation is under investigation. Potential explanations for the failure to identify candidate mutations in *avc3 and 5* include the possibility that the causative mutations reside in non-coding regions or unannotated coding sequence not included in the utilized exome capture design. *Avc4* and *6* were prioritized for further investigations (Table 1).

Avc4 carries a mutation in a dynein, axonemal, heavy chain 11 (*Dnah11*) gene

Avc4 caused AVSDs (Fig. 1A and B) and was previously mapped to a 11.5-Mb region on mouse chromosome 12 between *D12MIT181* and the distal end of chromosome 12 (8) (Table 1). Cardiac defects in addition to AVSD in *avc4* were previously reported (8). WES of a single *avc4* mutant predicted a homozygous missense mutation, T > C transition at g.117931223, within the *Dnah11* gene, encoding a dynein, axonemal, heavy chain 11

Table 1. Summary for mutations identified by WES in *avc* mutant lines obtained in forward genetic screen (8)

Line[a]	Chr	Marker 1	Marker 2	Mbp[b]	Nucleotide alterations[c]	AA alterations	Affected gene[d]	Predicted effect (probability)
avc1	5	*D5Mit229*	*D5Mit420*	3.6	Chr5: g.31265640A > G[e]	p.Arg841Glyfs*23[e]	*Ift172* Chr5:31253279-31291114	Mis-splicing, exon 24 skipping, a PTC in exon 25[e]
avc2	15	proximal end of chr5	*D15MIT267*	24.2	IP	IP	IP	IP
avc3	9	*D9Mit106*	*D9Mit302*	3.5	ND	ND	ND	ND
avc4	12	*D12Mit181*	distal end of chr12	11.5	Chr12:g.117931223T > C	p.Ser3630Pro	*Dnah11* Chr12:117877982-118199043	Missense; Deleterious (PROVEAN score: -4.717; PolyPhen-2 score: 0.999)
avc5	11	*D11Mit320*	*D11Mit245*	6.1	ND	ND	ND	ND
avc6	11	*D11Mit245*	*D11Mit360*	26.5	Chr11: g.87853328 C > T	p.Arg27*	*Mks1* Chr11:87853225-87863679	Non-sense; a PTC in exon 1; Deleterious (PROVEAN score: −3.249; PolyPhen-2 score: 0.997)

Using traditional Mendelian techniques and whole exome next generation sequencing, we have mapped mutations in four mouse lines with heritable CHD.

[a]mouse mutant lines generated by ENU-mutagenesis in forward genetic screen.

[b]candidate interval after mapping.

[c]for each line at least three controls (unaffected mice) and three mutants (affected mice) were sequenced, all mutations were absent in control animals.

[d]chromosomal location of the affected genes was determined using the December 2011 (GRCm38/mm10) assembly from UCSC.

[e]mutation described in Friedland-Little et al. (18); amino acids variations with a score equal to or below −2.5 [based on PROVEAN (80)] and above 0.85 [based on PolyPhen-2 (81,82)] are predicted to be deleterious. Abbreviations: avc, atrioventricular canal; Chr, chromosome; IP, in progress; ND, none detected; PTC, premature termination codon.

(Table 1). The *Dnah11* mutation was confirmed to be homozygous in E10 *avc4* mutant embryos by Sanger sequencing (Fig. 1C). The T > C transition resulted in a non-conservative amino acid change, p.Ser3630Pro, located in a highly conserved ATP-binding dynein motor region D5 of the DNAH11 protein (Fig. 1D). This change was predicted to be deleterious by PROVEAN (score: −4.717) and PolyPhen-2 (score: 0.999) (Table 1). To determine whether this mutation affected transcript stability, we performed qPCR on RNA isolated from E10 *avc4* wild-type and mutant embryos (three embryos/genotype). Similar levels of *Dnah11* expression were observed in both genotypes (1 ± 0.652 versus 1.072 ± 0.734, $P = 0.403$, Student's *t* test, Fig. 1E), suggesting that this mutation does not affect *Dnah11* transcript stability. We concluded that the phenotype observed in *avc4* mutant mice is due to *Dnah11* mutation, and refer to this allele as $Dnah11^{avc4}$.

Avc6 carries a mutation in Meckel syndrome, type 1 (*Mks1*) gene

Avc6 caused AVSDs (Fig. 1F and G) and was previously mapped to a 26.5-Mb region on mouse chromosome 11 flanked by *D11MIT245* and *D11MIT360* (8) (Table 1). Cardiac defects in addition to AVSD in *avc6* were previously reported in (8). WES of a single *avc6* mutant predicted a homozygous non-sense mutation, C > T transition at g.87853328, in the *Mks1* gene (Table 1). *Mks1* is a member of a class of B9 domain-containing proteins that is a component of the ciliary basal body (29–33). This mutation was subsequently verified as a true homozygous mutation using Sanger sequencing of E10 *avc6* embryos (Fig. 1H). The C > T transition results in an arginine being converted to a premature stop codon, p.Arg27* (Fig. 1I, Table 1; PROVEAN score: −3.249, PolyPhen-2 score: 0.997), that may lead to the synthesis of a truncated protein or to non-sense-mediated mRNA decay (NMD). To determine whether this mutation affected transcript stability, a qPCR analysis was performed on RNA isolated from E10 *avc6* control and mutant embryos (three embryos/genotype). Reduced but detectable *Mks1* expression was observed in *avc6* mutants (Fig. 1J, 1 ± 0.101 versus 0.708 ± 0.099, $P < 0.0001$). These data suggest that the aberrant *Mks1* transcript could undergo NMD. To directly test this hypothesis, we performed western blotting with an antibody against MKS1 on protein isolated from E10 *avc6* control and mutant embryos. *Avc6* mutant embryos expressed 23.69% of the amount of MKS1 compared with littermate wild-type controls, normalization to GAPDH (1.68 ± 0.109 versus 0.398 ± 0.235, P = 4.88E-05; Fig. 1K). We speculate that the small residual expression of wild-type-size MKS1 detected in *avc6* mutants may be due to translational read-through. We concluded that the phenotype observed in *avc6* mutant mice is due to *Mks1* mutation, and refer to this allele as $Mks1^{avc6}$.

$Mks1^{avc6}$ but not $Dnah11^{avc4}$ embryos have SHF Hh signaling defects

We investigated the mechanism underlying AVSDs in $Dnah11^{avc4}$ and $Mks1^{avc6}$ embryos. We asked whether either mutation abrogated SHF cilia-based Hh signaling, known to be required for AV septation (11–15). We observed that *Dnah11* expression was undetectable in the SHF or the heart tube during this process, at E10, by whole-mount *in situ* hybridization in wild-type embryos (Fig. 2A and B). *Dnah11* expression was observed in the forebrain, midbrain and hindbrain; regions known to have motile cilia (Fig. 2A and B). Although this result

Table 2. List of known mouse cilia genes mutations causing AVSD

Gene	Alleles	Location and MGI	AVSD/situs correlation	References
Dnaic1	*Dnaic1*$^{tm1.2Leo\ (c)}$; *Dnaic1*^{b2b1526Clo}; *Dnaic1*$^{b2b284Clo\ (a)}$	4A5, MGI:1916172	AVSD with heterotaxy only	(24,62,63,88–94)
Dnah5	*Dnah5*^{b2b002Clo}; *Dnah5*^{b2b016Clo}; *Dnah5*^{b2b601Clo}; *Dnah5*^{b2b1154Clo}; *Dnah5*^{b2b2395Clo}; *Dnah5*^{b2b1003Clo}; *Dnah5*$^{hlb612\ (a)}$;	15B1, MGI:107718	AVSD with heterotaxy only	(25,56,59,62,63,88,90–93,95–100)
Dnah11	*Dnah11*^{b2b1279Clo}; *Dnah11*^{b2b1727Clo}; *Dnah11*^{b2b2349Clo}; *Dnah11*$^{tm1Ssp\ (a)}$; *Dnahc11*$^{lrm3\ (a)}$; *Dnah11*$^{iv\ (a)}$	12F2, MGI:1100864	AVSD with heterotaxy only	(27,28,37,39,40,45,56,62,63,88,90,93, 96,101–107)
Ccdc39	*Ccdc39*^{b2b1735Clo}; *Ccdc39*$^{b2b2025.1Clo}$	3A3, MGI:1289263	AVSD with heterotaxy only	(62,63,88)
Drc1	*Drc1*^{b2b1654Clo}	5B1, MGI:2685906	AVSD with heterotaxy only	(62,63,88)
Hspb11/Ift25	*Hspb11*$^{tm1b(EUCOMM)Wti\ (c)}$; *Hspb11*$^{tm1a(EUCOMM)Wtsi,\ (c)}$;	4C7, MGI:1920188	AVSD without heterotaxy	(108,109)
Ift88	*Ift88*$^{cbbs\ (b)}$;	14C, MGI:98715	AVSD without heterotaxy	(110,111)
Ift172	*Ift172*$^{avc1(b)}$	5B1, MGI:2682064	AVSD without heterotaxy	(8,18,112)
Sufu	*Sufu*^{b2b273Clo},	19C3, MGI:1345643	AVSD without heterotaxy	(61–63,66,88)
Kif7	*Kif7*^{b2b2254Clo}; *Kif7*^{maki}; *Kif7*$^{tm1.1Hui\ (c)}$	7D2, MGI:1098239	AVSD without heterotaxy	(61–64,88,112)
Fuz	*Fuz*^{b2b1273Clo}; *Fuz*$^{gt/gt\ (b)}$	7B2, MGI:1917550	AVSD without heterotaxy,	(62,63,65,88,112–114)
Cntrl/Cep110	*Cntrl*^{b2b1468Clo}	2B-C1, MGI:1889576	AVSD without heterotaxy	(62,63,88)
Mks1	*Mks1*$^{avc6\ (b)}$;	11C11, MGI:3584243	AVSD without heterotaxy	(8) Fig. 1F and G, Supplementary Material, Table S1
Dync2h1	*Dync2h1*^{b2b414Clo}; *Dync2h1*$^{Gt(RRM278)Byg}$; *Dync2h1*^{lln}	9A1, MGI:107736	AVSD irrespective of heterotaxy	(62,63,88,112,115–117)
Mks1	*Mks1*^{hlb614}; *Mks1*$^{tm1a(EUCOMM)Wtsi\ (c)}$;	11C11, MGI:3584243	AVSD irrespective of heterotaxy	(29,31,32,69,72,73,98,118–124)
B9d1	*B9d1*$^{tm1a(EUCOMM)Wtsi\ (c)}$; *B9d1*$^{tm1d(EUCOMM)Wtsi\ (c)}$	11B2, MGI:1351471	AVSD irrespective of heterotaxy	(98,124–126)
Cc2d2a	*Cc2d2a*^{b2b1035Clo}	5B3, MGI:1924487	AVSD irrespective of heterotaxy	(53,62,63,88,98)
Nphp3	*Nphp3*$^{tm1Cbe\ (c)}$	9F1, MGI:1921275	AVSD irrespective of heterotaxy	(127)
Pskh1	*Pskh1*^{b2b1230Clo}	8D3, MGI:3528383	AVSD irrespective of heterotaxy	(62,63,88)
Tbc1d32	*Tbc1d32*^{b2b2284Clo}; *Tbc1d32*^{b2b2596Clo}; *Tbc1d32*$^{bromi\ (a)}$	10B3, MIM:2442827	AVSD irrespective of heterotaxy	(62,63,88,128)
Ift27	*Ift27*$^{tm1b(EUCOMM)Hmgu\ (c)}$	15E2, MGI:1914292	AVSD irrespective of heterotaxy	108, 109
Ift74	*Ift74*^{b2b796Clo}	4C5, MGI:1914944	AVSD irrespective of heterotaxy	(62,63,88,129,130)
Ift88	*Ift88*$^{fxo\ (b)}$; *Ift88*$^{tm1.1Bky\ (c)}$; *Polaris*$^{tm1Rpw\ (c)}$; *Ift88*$^{tm1Rpw\ (c)}$	14C, MGI:98715	AVSD irrespective of heterotaxy	(19,56,57,110–113,115,116,131–142)
Ift172	*Ift172*$^{wim\ (a)}$	5B1, MGI:2682064	AVSD irrespective of heterotaxy	(18,19,64,112,115–117)
Ift140	*Ift140*^{b2b1283Clo}	17A3.3, MGI:12146906	AVSD irrespective of heterotaxy	(62,63,88)

Alleles type: [(a)], null; [(b)], hypomorph; [(c)], targeted (null/knockout). Abbreviation: AVSD, atrioventricular septal defect.

Table 3. List of known human cilia genes mutations causing AVSD

Gene	Other aliases	Location and OMIM	Human syndrome	AVSD/situs correlation	References
DNAI1	*CILD1, DIC1, ICS1,*	9p13.3, OMIM:604366	PCD, Kartagener syndrome	AVSD with heterotaxy only	(23,42,59,90–93,95–97, 143–146)
DNAH5	*CILD3, DNAHC5*	5p15.2, OMIM:603335	PCD, Kartagener syndrome	AVSD with heterotaxy only	(23,42,59,90–97,143, 147–151)
DNAH11	*CILD7, DNAHC11*	7p21, OMIM:603339	PCD, Kartagener syndrome	AVSD with heterotaxy only	(36,37,41–44,59,90–93, 95–97)
MKS1	*MES, MKS, BBS13,*	17q22, OMIM:609883	Meckel-Gruber syndrome, type 1, (MKS1); Bardet-Biedl syndrome, type 13 (BBS13)	AVSD irrespective of heterotaxy	(32,33,46,57,58,67,69, 71–73,152–154)
MKKS	*KMS, MKS, BBS6*	20p12.2, OMIM:604896	Bardet-Biedl syndrome McKusick-Kaufman syndrome	AVSD irrespective of heterotaxy	(57,58,67,68,155–167)
EVC	*DWF-11, EVCL*	4p16.2 OMIM:604831	Ellis–van Creveld syndrome	AVSD irrespective of heterotaxy	(55,57,58,164,168–179)
EVC2	*LBN*	4p16.1 OMIM:607261			

Abbreviation: AVSD, atrioventricular septal defect; PCD, primary ciliary dyskinesia.

suggested that *Dnah11* was not required for the SHF Hh signaling, we directly evaluated *Hh* signaling in *Dnah11*^{avc4} mutants.

We quantitatively assessed the integrity of the Hh signaling pathway in *Dnah11*^{avc4} mutants by expression of Hh pathway target genes and biochemically. We first evaluated the Hh-dependent expression pattern of the Hh pathway genes *Gli1* and *Patched1 (Ptch1)*. Expression levels of *Gli1* and *Ptch1* reflect Hh signaling activity (18,34,35). SHF *Gli1* expression appeared qualitatively similar in wild-type and *Dnah11*^{avc4} mutant embryos at E10 by whole-mount *in situ* hybridization (Fig. 2C–F). *Gli1* and *Ptch1* expression in the posterior SHF (pSHF), microdissected at E10, were assessed quantitatively by qPCR. We found that *Gli1* and *Ptch1* transcription levels in the pSHF were statistically the same in wild-type and *Dnah11*^{avc4} embryos (1 ± 0.10 versus 0.98 ± 0.16, $P = 0.337$ for *Gil1*; 1 ± 0.11 versus 1.032 ± 0.20, $P = 0.279$ for *Ptch1*; Fig. 2G). Because the qPCR gene expression analysis required samples pooled from three distinct embryonic pSHFs, it remained feasible that individual sample variability in Hh signaling, that could explain the variable expression of AVSDs in *Dnah11*^{avc4} embryos, could have been masked. Therefore, we quantitatively assessed Hh signaling in individual thoracic samples by examining the proteolytic processing of the Gli3 transcription factor. In mammals, Gli3 exists in two forms, a full-length transcriptional activator (Gli3-190), and a proteolytically processed transcriptional repressor (Gli3-83). Processing of Gli3 from the full-length to the truncated form is regulated by Hh signaling and the ratio of Gli3-83/Gli3-190 is a quantitative measure of Hh signaling activity (18). We found that the Gli3-83/Gli3-190 ratio was statistically indistinguishable between individual wild-type and *Dnah11*^{avc4} embryos, with similar degrees of variability observed in both sample sets (1 ± 0.266 vs. 1.04 ± 0.240, for wild-type vs. *Dnah11*^{avc4}, respectively; Fig. 2H and I). No single *Dnah11*^{avc4} mutant embryo displayed a quantitative Hh signaling decrement that could cause an AVSD (18). These results supported the conclusion that *Dnah11*^{avc4} does not cause a decrement of SHF Hh signaling, and that *Dnah11*^{avc4} must affect AV septation by another mechanism.

In contrast, we observed a significant SHF Hh signaling defect in *Mks1*^{avc6} embryos. Strong SHF *Mks1* expression was observed at E10 by whole-mount *in situ* hybridization (Fig. 3A and B). We observed a severe decrement of the expression of Hh signaling target *Gli1* in the SHF of *Mks1*^{avc6} mutant embryos by whole-mount *in situ* hybridization at E10 (Fig. 3D and F versus C and E). This SHF *Hh* signaling defect provided a mechanistic explanation of the penetrant AVSDs observed in the *Mks1*^{avc6} line. *Mks1* expression was excluded from the developing heart in wild-type embryos (Fig. 3A and B), consistent with the required role for *Hh* signaling in SHF cardiac progenitors, not the heart, for AV septation (12).

Dnah11^{avc4} mutants demonstrated AVSDs only with disrupted laterality

Since *Dnah11*^{avc4} embryos demonstrated normal SHF *Hh* signaling, another deficit must have caused the observed AVSDs. We hypothesized that *Dnah11*^{avc4} caused AVSDs by cardiac isomerism resulting from laterality defects. *Dnah11* encodes a member of the cilia motility apparatus (36–38) and targeted disruption of the mouse *Dnah11* (*lrd*) gene results in randomization of laterality (37,39,40). *DNAH11* mutations in humans cause primary cilia dyskinesia (PCD) and Kartagener syndrome (36,41–44). The *Dnah11*^{avc4} mutation is distinct from the previously reported *Dnah11* mutations in both, mice (37,40,45) (Table 2) and humans (37,41,43,44) (Table 3). We investigated the relationship between *Dnah11*^{avc4}, AV septation, and body plan situs. 58% of *avc4* mutants (29/50; Supplementary Material, Table S1) demonstrated situs solitus and normal AV septation was observed in each situs solitus mutant (Supplementary Material, Table S1). Situs inversus totalis was observed in 24% of *avc4* mutant embryos (12/50; Supplementary Material, Table S1 and data not shown) and normal AV septation was observed in each situs inversus totalis mutant (Supplementary Material, Table S1). 18% of *avc4* mutants (9/50; Supplementary Material, Table S1 and data not shown) demonstrated abnormal situs with dextrocardia (4/9) and/or lung isomerism (6/9). AVSDs were present in all of these nine mutant embryos (Fig. 1B versus A; Supplementary Material, Table S1). Additionally, serial cardiac section analysis suggested atrial isomerism, with (i) venous valves that are a normal feature of the right atrium observed in both atria of mutant mice with AVSDs (right atrial isomerism, 3/9) (Fig. 1B versus A) or (ii) absence of venous valves in both atria of mutant mice with AVSDs (left atrial isomerism, 5/9, data not shown). Littermate wild-type control animals all demonstrated situs solitus and normal AV septation (14/14; Fig. 1A and data not shown). AVSDs in *avc4* mutant embryos were significantly

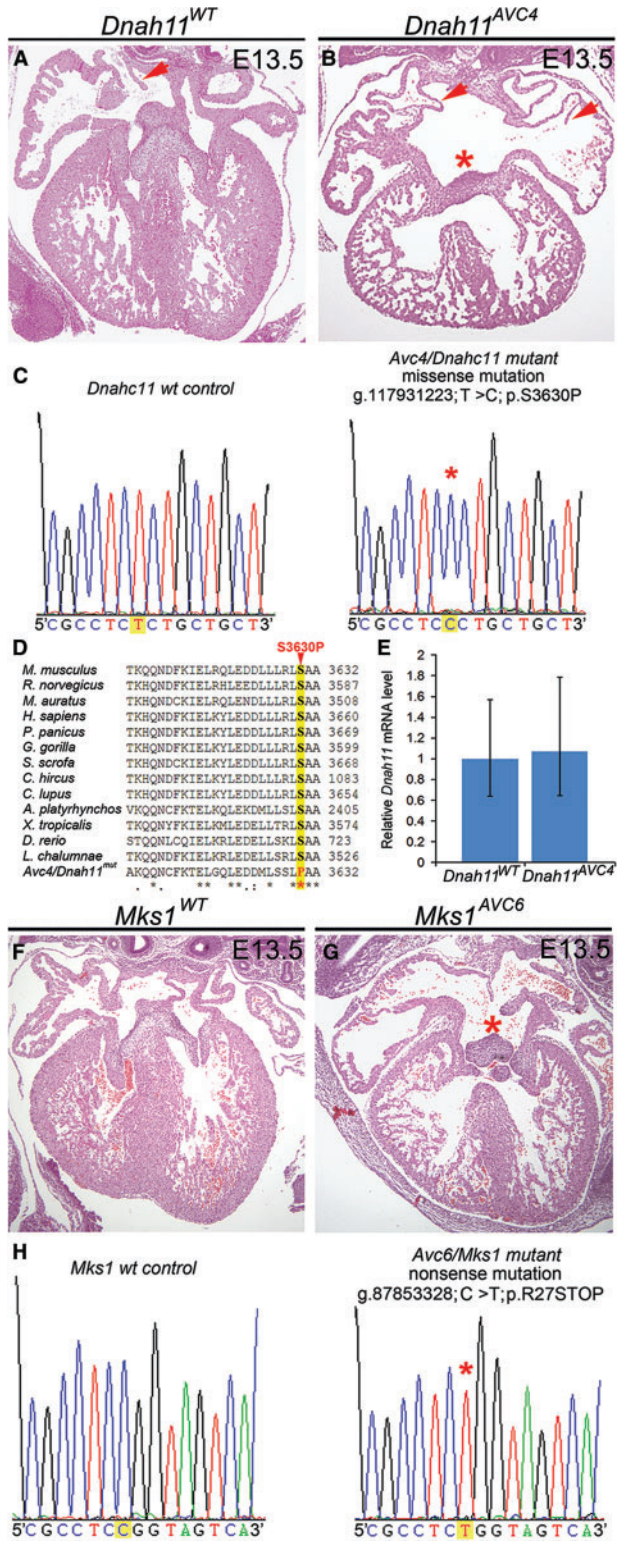

Figure 1. *Avc4* mouse line carries a recessive mutant allele of dynein heavy chain 11 (*Dnah11*) and *Avc6* mouse line carries a recessive mutant allele of Meckel syndrome, type 1 *(Mks1)*. **(A, B)** AVSDs in *avc4* mutant embryos correlate with ambiguous situs. Transverse sections of E13.5 *avc4* control **(A)** and mutant **(B)** hearts stained with hematoxilin and eosin. The *avc4* mutant shows a large AVSD (red asterisk). **(C)** Representative chromatograms from one E10 *avc4* wild-type (left panel C) and one E10 *avc4* mutant (right panel C) from Sanger sequencing of E10 *avc4* embryos (three embryos/genotype) confirmed the presence of homozygous missense mutation, T > C transition at g.117931223, within the *Dnah11* gene. Red asterisk indicates a position of base substitution. **(D)** This single base-pair mutation results in a non-conservative amino acid change, p.Ser3630Pro (highlighted), located in a highly conserved ATP-binding dynein motor region D5 of the DNAH11 protein. **(E)** *Dnah11* expression analysis by qPCR was performed on mRNA isolated from E10 *avc4* control and mutant embryos (three embryos/genotype). Similar levels of *Dnah11* expression were observed in both genotypes (mean ± SEM). **(F, G)** AVSDs in *avc6* mutant embryos. Transverse sections of E13.5 *avc6* control **(F)** and mutant **(G)** hearts stained with hematoxilin and eosin show AVSD (red asterisk) in 100% of examined mutants (28/28). No AVSDs were observed in wild-type littermates. **(H)** Representative chromatograms from one *avc6* wild-type (left panel H) and one *avc6* mutant (right panel H) from Sanger sequencing of E10 *avc6* embryos (three embryos/genotype) confirmed the presence of homozygous non-sense mutation, C > T transition at g.87853328, in the *Mks1* gene of *avc6* mutant mice. Red asterisk indicates a position of base substitution. **(I)** This single base-pair mutation results in an arginine (conserved across species) being converted to a premature stop codon, p.Arg27* (highlighted). **(J)** *Mks1* expression analysis by qPCR was performed on mRNA isolated from E10 *avc6* control and mutant embryos (3 embryos/genotype). Reduced but detectable *Mks1* expression was observed in *avc6* mutant embryos (1 ± 0.101 versus 0.708 ± 0.099, $P < 0.0001$, Student's *t* test). (K) Western blotting with an antibody against MKS1 on protein isolated from E10 *avc6* control and mutant embryos. *Avc6* mutant embryos expressed 23.69% of the amount of MKS1 compared with littermate wild-type controls after normalization to GAPDH (1.68 ± 0.109 versus 0.398 ± 0.235, $P = 4.88E\text{-}05$, Student's *t* test). Data are mean ± SD. Magnification: (A, B and F, G) = 40×. The red arrowheads indicate presence of venous valve. Abbreviations: AVSD, atrioventricular septal defect; *avc4*, atrioventricular canal 4 line; *avc6*, atrioventricular canal 6 line.

Figure 1. Continued

associated with abnormal or ambiguous situs (Fisher's Exact Test (FET), $P < 0.0001$, Supplementary Material, Table S1).

Mks1^{avc6} embryos demonstrated AVSDs independent of laterality defects

Mks1 encodes a centrosomal protein required for primary cilium formation (30–33) and has been previously implicated in left-right patterning of mouse and human embryos (29,33) (Tables 2 and 3). The mutation found in *avc6* mouse line has not been previously reported among *Mks1* mutations in mice (29,31) (Table 2) or humans (30,33,46–48) (Table 3). We investigated the relationship between *Mks1*^{avc6}, AV septation, and body situs. 89% of *avc6* mutant embryos demonstrated situs solitus (25/28; Supplementary Material,

Table S1 and data not shown), whereas 11% of *avc6* mutants showed abnormal situs with dextrocardia (3/28; Supplementary Material, Table S1 and data not shown). AVSDs were present in 100% of mutant embryos (28/28; Supplementary Material, Table S1, Fig. 1G versus F, and data not shown). All *avc6* wild-type control littermate embryos showed situs solitus with normal AV septation (12/12, Fig. 1F, and data not shown). These results demonstrated that $Mks1^{avc6}$ causes AVSDs independent of L/R defects (FET, $P > 0.05$, Supplementary Material, Table S1) since there was no observed association between heterotaxy and AVSDs in this line (FET, $P > 0.05$, Supplementary Material, Table S1).

Cilia structural genes and signaling genes, but not cilia motility genes are expressed in the SHF

Our analysis of *avc4*, *avc6* and previously *avc1*, suggested a correspondence between the class of cilia mutation, SHF gene expression and SHF Hh signaling. Specifically, *Dnah11*, a cilia motility gene, was not expressed in the SHF nor required for SHF Hh signaling whereas *Mks1* and *Ift172*, primary cilia structural genes, were both expressed in the SHF and required for SHF Hh signaling. We asked whether this pattern of cilia gene expression was indicative of a general pattern such that the subcategory of cilia gene action predicted its SHF gene expression and requirement for SHF Hh signaling. To interrogate SHF expression of cilia genes in an unbiased manner, we performed RNA-seq on the embryonic pSHF, containing AV septum progenitors. We isolated the pSHF by microdissection from mixed background wild-type embryos at E9.5 (49). Sufficient RNA was collected by pooling the pSHF from three embryos per sample and RNA-seq was performed in quintuplicate, with each library sequenced to a depth of 17–26 million reads.

We found that genes encoding components of the cilia motility machinery were expressed at low or absent levels whereas genes encoding components of the primary cilia or cilia signaling were expressed at high levels in the SHF (Fig. 4, Supplementary Material, Table S2). Specifically, we examined the expression of the 13 axonemal dynein orthologues essential for cilia motility and whose mutations disturb L/R axis formation. We found that 12/13 cilia motility genes were negligibly expressed in the SHF (range: undetectable to 41 ± 16) consistent with transcriptional noise or absent expression (Fig. 4A and B, Supplementary Material, Table S2), utilizing an expression threshold composed of genes previously examined by in-situ hybridization and RT-PCR and defined as not expressed in the pSHF (e.g. *Hoxb8*, *Hoxc8*, *Hoxd8* (50) at 41 ± 9, 5 ± 3 and 8 ± 5, respectively). In contrast, we examined the expression of cilia genes encoding intraflageller transport proteins (IFTs), required for primary cilia structure and function essential for cilia-based signaling. We found that 15/15 IFT genes identified in the ciliome database (http://www.sfu.ca/~leroux/ciliome_database.htm) (51) and detected in our RNA-seq were highly expressed in the SHF (range: 87 ± 27 to 857 ± 93) (Fig. 4A and B, Supplementary Material, Table S2). The high levels of transcript reads of the IFT genes were comparable to genes previously examined and defined as highly expressed in the pSHF (e.g. *Osr1* (11), and *Foxf2* (49) at 1012.7 and 284.5, respectively). These observations demonstrated that the class of cilia genes specific to cilia motility, whose mutations disturb L/R axis formation, are not expressed in the SHF and are therefore unlikely to be required for SHF Hh signaling, whereas all primary cilia genes are strongly expressed in the SHF and may facilitate SHF Hh signaling.

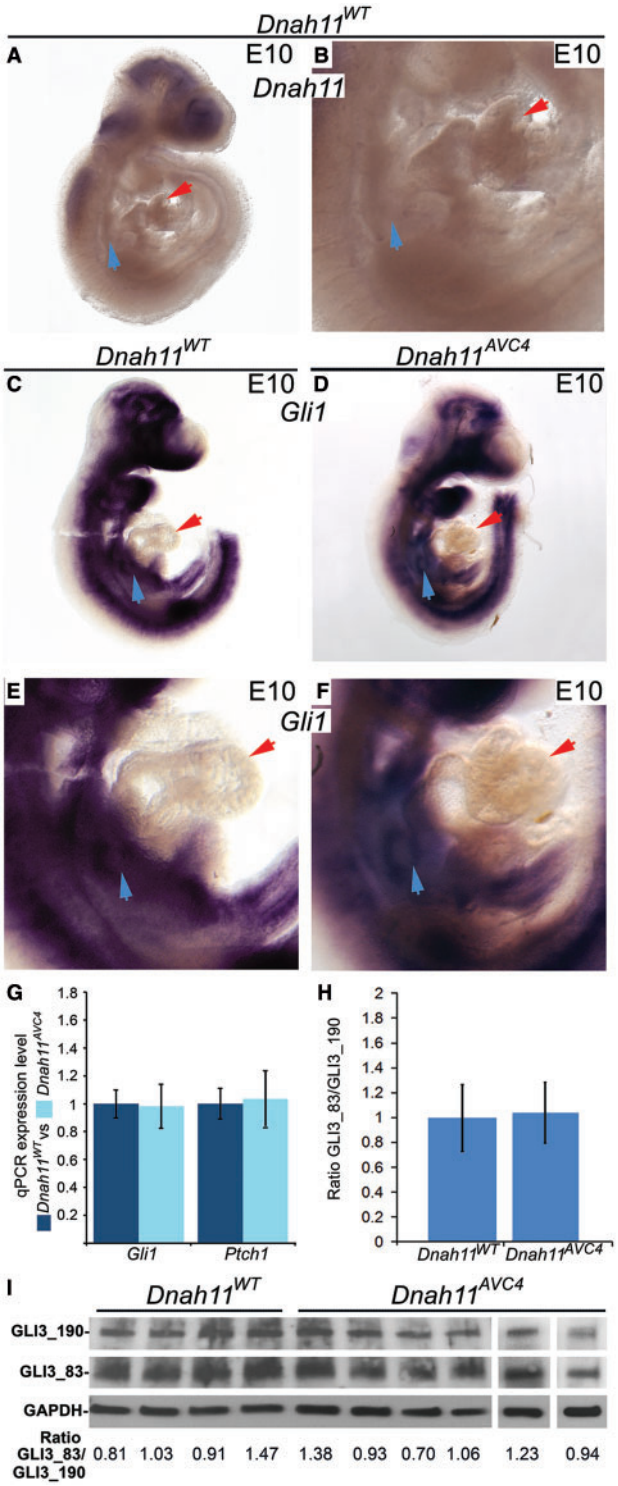

Figure 2. $Dnah11^{avc4}$ embryos do not have SHF Hh signaling defects. **(A, B)** Expression of *Dnah11* analysed in E10 wild-type embryos by whole-mount *in situ* hybridization. *Dnah11* expression was undetectable in the SHF (blue arrowhead) and the heart tube (red arrowhead) in E10 wild-type embryos (A, B) but it was observed in the forebrain, midbrain, and hindbrain, regions known to have motile cilia (A, B). Expression of *Gli1* analysed in E10 $Dnah11^{avc4}$ control **(C, E)** and mutant **(D, F)** embryos by whole-mount *in situ* hybridization. Similar levels of *Gli1* expression were observed in both genotypes. The blue arrowheads indicate the SHF and the red arrowheads—the heart. **(G)** *Gli1* and *Ptch1* expression analysis by qPCR was performed on mRNA isolated from SHF microdissected from E10 $Dnah11^{avc4}$ wild-type and mutant embryos. Similar levels of Gli1 and *Patch1*

AVSDs are a common feature in mice and humans with cilia mutations

Our analysis of *avc1* (8,18), *avc4* and *avc6* indicated a strong relationship between AVSD causation and cilia gene mutations. We reviewed the mouse and human cilia literature to determine whether there was an association between cilia gene mutations and AVSDs, including primum ASDs, inlet VSDs, common atrium, and complete common AV canal. Review of the mouse cilia literature showed that cilia mutations commonly caused AVSDs. Specifically, we identified 22 cilia genes with alleles that caused AVSDs as part of the phenotypic spectrum (Table 2). Human ciliopathies are a group of over 100 overlapping clinical disorders caused by defects in the cilium and its anchoring structure, the basal body (52–57). We found that specific human ciliopathy mutations, including those causing Ellis–van Creveld, McKusick-Kaufman, Bardet-Biedl type 13, Meckel-Gruber, and Kartagener syndrome (58), were commonly associated with AVSDs (Table 3).

AVSDs/heterotaxy correspondence in humans and mice with cilia gene mutations is predicted by SHF gene expression

We hypothesized that AVSD/heterotaxy concordance caused by cilia gene mutations would be predicted by the cilia gene's SHF gene expression. We compared the SHF RNA-seq expression values of the 26 cilia genes associated with AVSDs in mice and humans (Tables 2 and 3) with the AVSD/heterotaxy phenotypic concordance caused by their mutations (Fig. 4A and C, Supplementary Material, Table S1), and validated the relative pSHF expression for 22 by qPCR (Fig. 4D). AVSDs caused by mouse or human mutations in cilia genes with roles selective to cilia motility (e.g. *Dnaic1, Dnah5* or *Dnah11* in mice and *DNAH5* [MIM: 603335] or *DNAH11* [MIM: 603339] in humans) were presented only concurrently with heterotaxy syndrome (Tables 2 and 3). We found that the SHF expression for these cilia genes was low or undetectable (Fig. 4). In contrast, AVSDs caused by cilia mutations affecting the Hh signaling were observed without heterotaxy or irrespective of heterotaxy (Table 2). Cilia genes whose mutations caused AVSD without or irrespective of heterotaxy were strongly expressed in the SHF. Expression of cilia genes whose mutations caused AVSDs only with heterotaxy was significantly lower than that for cilia genes whose mutations caused AVSD either without heterotaxy or irrespective of heterotaxy (Kruskal-Wallis H stat = 12.16, $P = 0.0023$; AVSD with heterotaxy only versus AVSD without heterotaxy ($P = 0.0336$) and AVSD with heterotaxy only versus AVSD irrespective of heterotaxy ($P = 0.0016$)) (Fig. 4A and C). These results demonstrated perfect concordance between SHF gene expression and the pattern of AVSDs and heterotaxy syndrome presentation in mice and humans with cilia mutations.

Discussion

We report the genetic basis of AVSDs in two ENU-induced mutant mouse lines, *avc4* and *avc6*. A *Dnah11* mutation segregated with AVSDs in line *avc4*, and a *Mks1* mutation segregated with AVSDs in line *avc6*. Because these mutations were the only homozygous mutations identified in embryos demonstrating recessive AVSDs, we conclude that $Dnah11^{avc4}$ is causative of AVSDs in line *avc4* and that $Mks1^{avc6}$ is causative of AVSDs in line *avc6*. These cilia gene mutations join the identification of *Ift172* mutation in *avc1* (18), defining cilia gene mutations as causative of AVSDs in three murine *avc* lines analysed to date. Cilia gene mutations are not a well-appreciated cause of AVSDs, perhaps because AVSD presentation is part of a complex group of phenotypes often observed in ciliopathies. Nonetheless, our review of the literature identified mutations in 22 mouse cilia genes and 7 human cilia genes with AVSDs described as part of the phenotypic spectrum. These observations suggest that

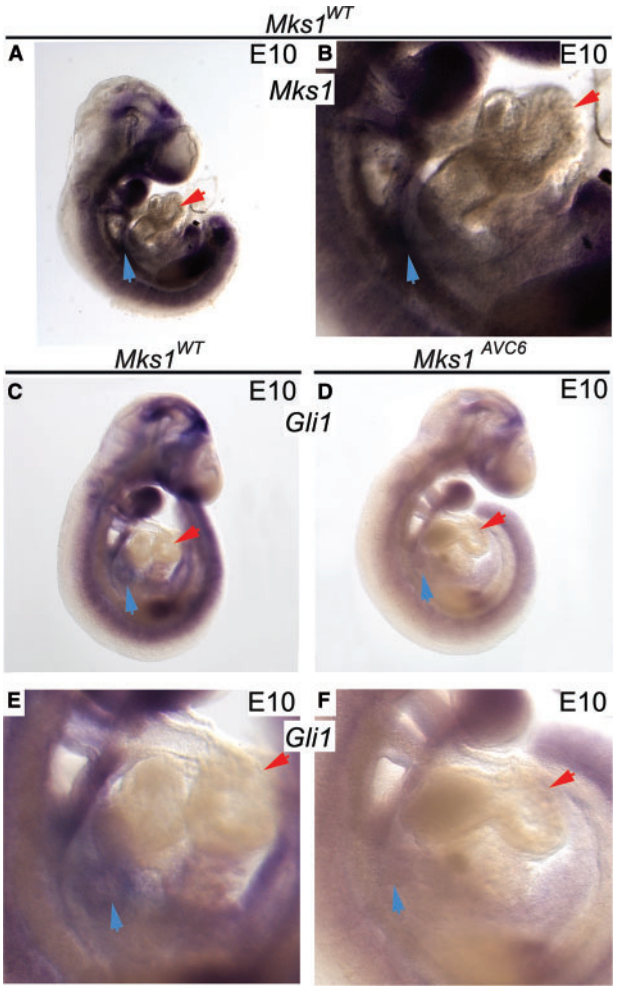

Figure 3. $Mks1^{avc6}$ embryos have SHF Hh signaling defects. **(A, B)** Expression of *Mks1* analysed in E10 *avc6* wild-type embryos by whole-mount *in situ* hybridization. *Mks1* was expressed in the SHF (blue arrowhead) but not in the heart tube (red arrowhead) in E10 *avc6* wild-type embryos **(A, B)**. Expression of *Gli1* analysed in E10 $Mks1^{avc6}$ control **(C, E)** and mutant **(D, F)** embryos by whole-mount *in situ* hybridization. A severe qualitative decrement of *Gli1* expression was observed in the SHF of $Mks1^{avc6}$ mutant embryos. The blue arrowheads indicate the SHF and the red arrowheads – the heart. Magnification: 40×. Abbreviations: *avc6*, atrioventricular canal 6 line; SHF, second heart field.

expression were observed in both genotypes (1 ± 0.10 versus. 0.98 ± 0.16, $P = 0.337$ for *Gli1*; 1 ± 0.11 versus 1.032 ± 0.20, $P = 0.279$ for *Ptch1*, Student's *t* test). Full-length (Gli3–190) and processed (Gli3–83) forms of Gli3 were detected by western blot in $Dnah11^{avc4}$ wild-type and mutant embryos **(H,I)**. The Gli3-83/Gli3-190 ratio was statistically indistinguishable between individual $Dnah11^{avc4}$ wild-type and mutant embryos, with similar degrees of variability observed in both sample sets (1 ± 0.266 versus 1.04 ± 0.240, for wilt-type vs. $Dnah11^{avc4}$, respectively, $P = 0.874$, Student's *t* test) **(H, I)**. Data are mean ± SD. Magnification: (A–F) = 40×. Abbreviations: *avc4*, atrioventricular canal 4 line; SHF, second heart field.

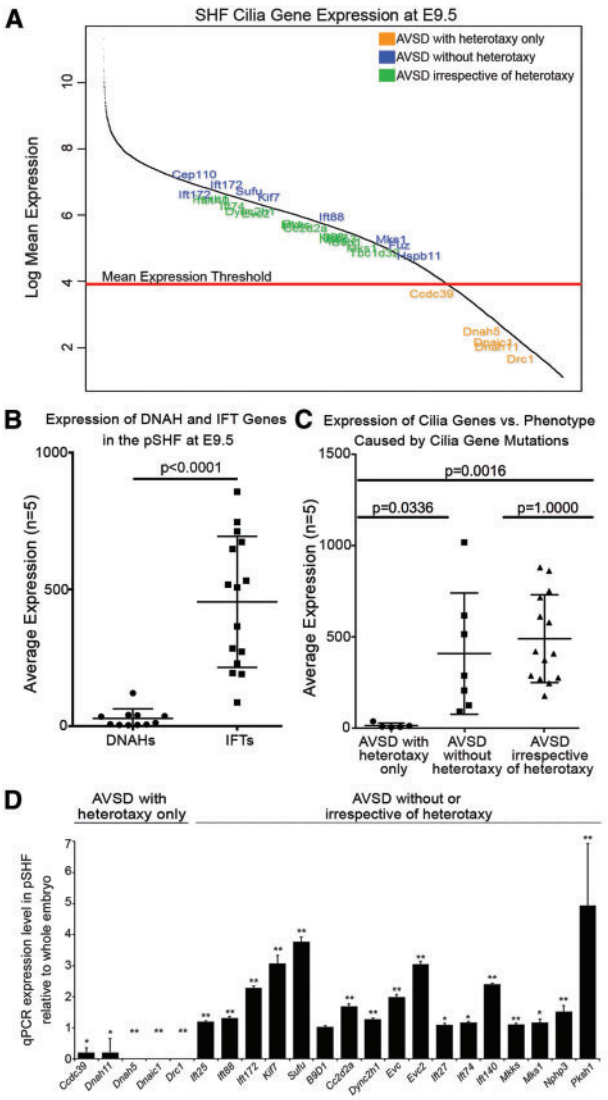

Figure 4. Cilia structural genes and cilia signaling genes, but not cilia motility genes, are expressed in the SHF. **(A)** All genes detected by RNA-seq plotted by log (mean expression), with genes from Tables 2 and 3 labeled by phenotypic classes (orange, AVSD with heterotaxy only; blue, AVSD without heterotaxy; green, AVSD irrespective of heterotaxy). Genes below a normalized mean expression *n* of 50 fall within low-level transcriptional noise. **(B)** Graph of *Dnah* and *Ift* cilia genes expressed by respective normalized FPKM. **(C)** Graph of all cilia genes expression by phenotypic class with respective normalized FPKM. **(D)** qPCR expression analysis of 22 cilia genes associated with AVSD in mice and humans (Tables 2 and 3) was performed on mRNA isolated from E9.5 wild-type whole mouse embryo and pSHF. Low expression of cilia genes whose mutations caused AVSD with heterotaxy only was observed in contrast to high expression of all of the genes whose mutations caused AVSD without heterotaxy or AVSD irrespective of heterotaxy. qPCR data are mean ± SD, $n = 3$, $^{*}P < 0.01$, $^{**}P < 0.001$, Student's *t* test.

although not responsible for all AVSDs, mutations in cilia genes may play an important role in AVSD causation.

Primary and motile cilia are both required for L/R determination (54,55,57). Furthermore, our findings suggest that primary cilia but not motile cilia are required for SHF Hh signaling (Figs. 2 and 3). Based on these two distinct cilia-based processes, we generated a model that predicted three classes of cilia gene mutations causing distinct expression of AVSDs and heterotaxy (Fig. 5): (i) Mutations that affect laterality but not SHF Hh signaling; (ii) mutations that affect SHF Hh signaling but not laterality; and (iii) mutations that affect both laterality and SHF Hh signaling. We found that the phenotypic expression of mutant mouse alleles from our forward genetic screen and more generally from mouse and human cilia alleles described in the literature (Tables 2 and 3) support this model, as detailed below.

The model (Fig. 5) predicts that mutations of cilia genes with roles specific to cilia motility would present AVSDs only concurrently with heterotaxy. In this report, we found that AVSDs in *Dnah11*^{avc4} mutant mice occurred only with heterotaxy (Figs 1A, B and 5, Table 2, Supplementary Material, Table S1). Mutations of *Dnah11* or other genes specifically required for cilia motility, such as *Dnaic1 and Dnah5*, cause randomized L/R patterning (24,25,27,28,37,39,40). Mutations in their human orthologues cause Primary Ciliary Dyskinesia (PCD), a disorder also characterized by decreased or absent cilia movement, including respiratory morbidity and impaired male fertility (23,36,37,42–44,59). PCD patients can present with normal or inverted laterality (e.g. Kartagener Syndrome) or heterotaxy syndrome (37,41–44,59). AVSDs were only observed in PCD patients with heterotaxy syndrome, not in humans with PCD or in mice with mutations in cilia motility genes when normal or perfectly inversed situs was present (36,37,42–44,59), (Tables 2 and 3, Supplementary Material, Table S1) analogous to the AVSDs observed in the *Dnah11*^{avc4} line (Fig. 1B, Table 2, Supplementary Material, Table S1). These observations imply that cilia motility genes are not required for SHF Hh signaling, otherwise mutations in this class of cilia gene would cause penetrant AVSDs regardless of their impact on situs. In this report, we found that *Dnah11* is not expressed in the SHF (Fig. 2A and B) and *Dnah11*^{avc4} does not disrupt SHF Hh signaling (Fig. 2C–I). Remarkably, we also observed that the entire cohort of dynein heavy chains and other genes specifically required for cilia motility is negligibly expressed in the SHF (Fig. 4, Supplementary Material, Table S2). These observations provide direct evidence that the cilia motility machinery is not required for SHF Hh signaling.

The perfect correspondence between AVSDs and L/R abnormalities caused by mutations of cilia genes required specifically for cilia motility implies that AVSDs result from situs abnormalities in these cases. The atrial septum is derived entirely from the left side of the wild-type SHF, demonstrated by its inclusion in the fate map of the left-sided marker *Pitx2* (60). It is therefore not surprising that mutations causing heterotaxy or sidedness defects concomitantly affect the development of this 'sided' structure (Supplementary Material, Table S1 and reference (27)). The molecular basis of the AVSDs caused by heterotaxy awaits future investigation, although this study appears to rule out a role for SHF Hh signaling defects.

The model (Fig. 5) predicts that mutations in cilia genes with a selective role in Hh signaling but not laterality would be predicted to cause AVSDs without heterotaxy (Fig. 5). This cohort includes reported mutations in *Sufu* and *Kif7* (61–66) (Tables 2 and 3).

The model (Fig. 5) predicts that mutations in cilia genes that affect Hh signaling and L/R determination would cause AVSDs irrespective of heterotaxy (Fig. 5). This group includes mutations in multiple intraflagellar transport genes, such as *Ift88*^{tm1Rpw} (Polaris) and other genes that affect primary cilia function. This class of mutations causes defective Hh signaling, resulting in AVSDs in all cases, and defective L/R determination, resulting in randomized laterality and heterotaxy in some cases. The independent effect of these cilia gene mutations on SHF Hh

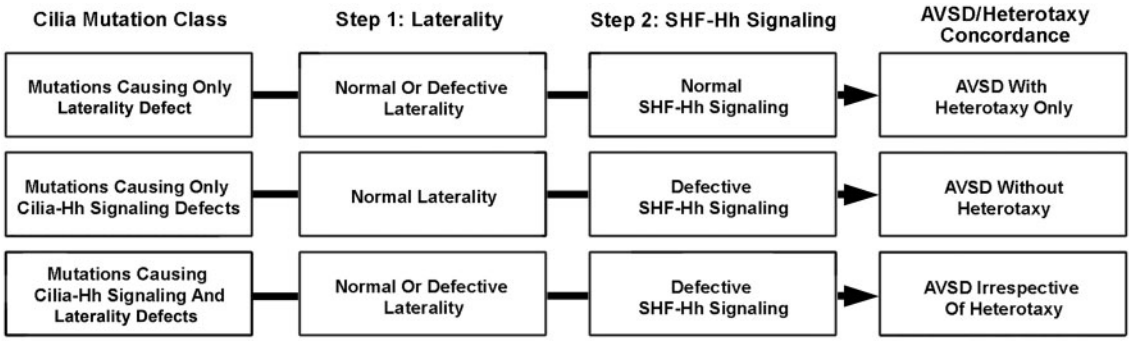

Figure 5. Three classes of cilia mutations with distinct effects on laterality and Hh signaling cause distinct presentations of AVSDs and heterotaxy. Class 1 mutations affect cilia motility (resulting in disruption of correct L/R axis formation) but not AV septum progenitors. Mutations in this class, such as *Dnah11*^{avc4}, only cause AVSDs secondary to abnormal situs, when present. Class 2 mutations affect signaling but not laterality. Mutations of this class, such as *Ift172*^{avc1} or *Mks*^{avc6}, disrupt AV septum progenitors causing AVSDs but not situs abnormalities. Class 3 mutations disrupt both cilia motility and signaling. Mutations of this class, such as *Polaris*, disrupt laterality and AV septum progenitors and cause AVSDs irrespective of situs abnormalities. This three-class model accurately fits the phenotypic variance of AVSDs and heterotaxy observed in humans and mice with cilia gene mutations.

signaling and L/R determination uncouples the phenotypic expression of AVSDs and heterotaxy.

Interestingly, a select group of mutations in genes with roles in both Hh signaling and laterality also cause AVSDs without affecting laterality. For example, although *Mks1* is required for ciliogenesis and Hh signaling, and severe *Mks1* mutations cause both laterality and Hh signaling defects in mice (29,31), we observed that the *Mks1*^{avc6} allele significantly caused AVSDs (28/28) but not heterotaxy (3/28; $P > 0.05$) (Figs. 1F, G and 5, Supplementary Material, Table S1). *Mks1* is expressed in the SHF at E10 (Fig. 3A and B) and is required for SHF Hh signaling (Fig. 3C–F). These observations suggest that the *avc6* allele of *Mks1* is hypomorphic, perhaps explained by the small amount of residual wild-type-sized MKS1 observed in *avc6* mutant embryos (Fig. 1K). Thus, *Mks1*^{avc6} affects SHF Hh signaling with high penetrance but L/R axis determination with much lower penetrance. In humans, the literature demonstrates an allelic series of *Mks1* mutations; more severe *Mks1* mutations cause both AVSDs and situs abnormalities whereas milder mutations cause AVSDs in the absence of situs abnormalities (29,31–33,46–48,67–73). We also observed this pattern among *Ift172* alleles in mice: *Ift172*^{avc1}, a hypomorphic allele, caused Hh signaling but not situs defects (18) whereas *Ift172*^{wim}, a protein-null, caused Hh signaling and situs abnormalities (19). These observations suggest that for the genes that contribute to primary cilia function, the requirement for Hh signaling may be more dosage-sensitive than the requirement for L/R determination. The molecular basis for this distinction is currently unclear. It is possible that cilia in the node and the SHF may have distinct structural or signaling properties. Based on these examples, we speculate that hypomorphic mutations of the large number of genes that contribute to primary cilia structure and signaling may contribute to human simplex AVSDs.

The relationship between cilia gene mutations and the genetic underpinnings of human simplex AVSDs, the most common form of AVSDs in CHD, awaits future studies. *A-priori*, our model predicts that mutations affecting cilia-based Hh-signaling, but not laterality, likely predominate. The first single-gene risk factor for simplex AVSD in humans, *CRELD1* (74), encodes a cilia-localized protein. Consistent with our model, CRELD1 does not appear to be required for L/R determination, since *Creld1* null mice do not manifest L/R abnormalities (75), suggesting that *CRELD1* mutations contribute to the cause of AVSD through disruption of SHF Hh signaling rather than cilia motility. Our findings coalesce with previous literature to provide a conceptual scaffold for understanding the pleiotropic effects of cilia gene mutations in human CHD. We speculate that cilia gene mutations will contribute to simplex AVSDs in humans. We also suggest that AVSDs should be considered as a part of the ciliopathy spectrum and that the clinical sequela of impaired cilia function be considered in the evaluation of patients with AVSDs.

Materials and Methods

Mouse strains

Avc1–Avc6 mouse lines were identified in a screen for recessive ENU-induced mutations that caused prenatal lethality and structural heart defects (8). All experiments employed age-, gender- and genetic strain-matched controls to account for any variations in data sets compares across experiments. All experiments were performed under the University of Chicago Institutional Animal Care and Use Committee (IACUC) approved protocol (ACUP no. 71737) and in compliance with the USA Public Health Service Policy on Humane Care and Use of Laboratory Animals.

WES analysis

Exome captures were performed on mouse genomic DNA using a hybrid capture reagent from Roche Nimblegen (SeqCap EZ Mouse Exome SR; 54.3 Mb target including 203 225 exonic regions (C57BL/6J, NCBI37/mm9); described in Fairfield *et al.* (76). Library construction, hybrid capture and sequencing were performed as described in Fairfield *et al.* (76) and Buchovecky *et al.* (77), with sample indexes incorporated prior to capture. All sequencing of post-enrichment shotgun libraries was performed on an Illumina GA2x, with paired-end 76-p reads (PE76), and a third read to determine the index sequence associated with each read-pair. Sequence reads were mapped to the mm9 reference genome with BWA (78), and then separated by sample based on the index sequence. Variants were called with SAMtools (79). Custom scripts were used to annotate variants with respect to their predicted impact on protein sequence. To remove inbred strain polymorphisms as well as systematic sequencing artifacts, we removed from consideration variants identified in any of the other strains described here or 10 other

mice representing unrelated phenotypes. Exome sequencing identified 2973 exonic variants for *avc2*, 25 920 for *avc3*, 3532 for *avc4*, 2400 for *avc5* and 24 331 for *avc6* mutants. Strain-specific homozygous, protein-altering (missense, non-sense, canonical splice and coding indel) variants within the mapping interval were identified and subjected to Sanger confirmation.

Sanger validation of candidate mutations

Candidate mutations were validated by PCR amplification and sequencing of affected and unaffected samples from the mutant colonies (76). Briefly, genomic DNA (6 ng) was amplified in a 50 μl PCR reaction with 100 nM of specifically designed primers near the mutation site and 25 μl of Taq 2× master mix (New England Biolabs) at 94 °C for 3 min, followed by 35 cycles of 94 °C for 30 s, 57 °C for 30 s and 72 °C for 30 s, and final extension at 72 °C for 5 min. The PCR products were then purified with Qiaquick columns (Qiagen), and sent for sequencing to the University of Chicago Sequencing Facility. Primer sequences used in this study are listed in Supplementary Material, Table S3.

Interpretation of novel missense single nucleotide variations (SNVs)

To predict whether the candidate SNVs would have deleterious effects or not, we used 2 software programs, i.e., Protein Variation Effect Analyzer (PROVEAN; J. Craig Venter Institute, San Diego, California, USA, http://http://provean.jcvi.org/index.php) (80) and Polymorphism Phenotyping v2 (PolyPhen-2; Harvard University, Cambridge, Massachusetts, US, http://genetics.bwh.harvard.edu/pph2) (81,82). PROVEAN uses sequence homology to predict amino acid substitutions that will affect protein function, thus contributing to a disease (80). PROVEAN predicts substitutions with a score ≤ -2.5 as being 'deleterious', and with a score above the threshold -2.5 as being 'neutral'. PolyPhen-2 takes into account the physicochemical characteristics of the wild-type and mutated amino acid residue and the consequence of the amino acid change for the structural properties of the protein in addition to evolutional conservation (81,82). PolyPhen-2 generates a different scale of reported scores, with the corresponding predictions being 'probably damaging' with a score larger than 0.85, 'possibly damaging' with a score between 0.85 and 0.15, and 'benign' with a score <0.15. Because PolyPhen-2 considers only human protein sequences, the mouse SNVs were investigated in the context of human protein sequences.

Histology

Embryos harvested at E13.5 were flushed with cold PBS, genotyped and fixed overnight at 4 °C in 4% paraformaldehyde (Sigma-Aldrich). Subsequently, they were processed for paraffin-embedded sections and analysed by H&E staining according to the manufacturer's protocol (Sigma-Aldrich).

RNA isolation and RT-PCR

To examine the effect of mutations on transcripts, we extracted total RNA from control and mutant E10 embryos using RNeasy Mini Kit (Qiagen) according to the manufacturer's protocol. Reverse transcription reaction was performed using the SuperScript III First-Strand Synthesis SuperMix for quantitative RT-PCR (Invitrogen) according to the manufacturer's recommendations. RT-PCR was performed using the POWER SYBR Green PCR master mix from Applied Biosystems and run on an Applied Biosystems AB7500 machine in 96 well plates. The relative gene expression level was calculated by the ΔΔCt method (83) using glyceraldehyde-3-phosphate dehydrogenase (*Gapdh*) gene expression level as internal control. The data presented are the average of three independent experiments. Primer sequences used in this study are listed in Supplementary Material, Table S3.

In situ hybridization

Whole-mount RNA *in situ* hybridization was performed as described previously (84). Briefly, sense and antisense probes were generated using a digoxigenin (DIG) RNA labeling kit (Roche). Probes were hybridized overnight at 65 °C with E10 wild-type embryos. DIG-labeled probes were detected by anti-digoxin-AP Fab fragments (Roche) and precipitated by BM purple AP substrate (Roche). Primer sequences used to generate *Dnah11* and *Mks1* ISH probes are listed in Supplementary Materials, Table S3. The *Gli1* ISH probe was a kind gift from Dr Elizabath Grove (University of Chicago, Chicago, IL, USA).

Western blotting

Western blots were performed in sextuplicate, Detection of GLI3 and MKS1 protein was performed according to standard procedures (18) using a polyclonal rabbit anti-GLI3 antibody (sc-20688; Santa Cruz Biotechnology, Santa Cruz, CA) and polyclonal rabbit anti-MKS1 antibody (16206-1-AP; Proteintech Group Inc., Chicago, IL).

RNA-seq data analysis

Total RNA was extracted from the pSHF as described previously in (49), and five libraries were generated by pooling 3 samples per library (TruSeq RNA Sample prep kit v2; Part no. RS-122-2001). 51-bp single-ended sequencing libraries were prepared and sequenced using the Illumina HiSeq2500 platform by the Genomics Core Facility at the University of Chicago (Invitrogen, 2013). We focused on the 38-bp reads on the right-side with a general declining pattern of quality scores as expected and ensured a larger than 30 quality score per base. Around 17-26 million RNA-seq reads were generated for each replicate and aligned to the GRCm38/mm10 build of the *Mus musculus* genome using TopHat v2.0.6 (85). Gene-level expression was quantified as read counts per exon using featureCounts in the Bioconductor package SubRead (86). Reads overlapping exons in annotation build 38.1 of NCBI RefSeq database were included. Counts were converted to log2 counts, fit to a generalized linear model across five wild-type replicates and six mutant samples (data not shown), and normalized to a gene- and sample-specific normalization factor generated by the model with the DESeq2 package (87).

Normalized gene expression values from wild-type E9.5 pSHF RNA-seq data ($n = 5$) was retrieved for all genes in Figure 5A. For the subcategory of cilia genes, statistical differences in expression level between the DNAHs and IFTs were evaluated through the Mann-Whitney U-test, and for the 26 cilia genes associated with AVSD, the between class statistical differences in expression level according to mutant phenotype were evaluated through the Kruskal-Wallis test followed by Dunn's multiple

comparisons test using GraphPad Prism version 6.05 (GraphPad Software, La Jolla CA, USA).

Statistics

Values are shown as the mean ± SD of the indicated number of measurements. Statistical significance was determined using Student's *t*-test (two-tailed) with a significance of 0.05 or FET. No statistical method was used to predetermine sample size, and the animal experiments were not performed in a blinded fashion. Mice were assigned at random to treatment groups for all mouse studies.

Supplementary Material

Supplementary Material is available at *HMG* online.

Authors' Contributions

IPM and OBT conceived and designed the study; OBT, JDS, LF, AK, JK and MP performed wet lab experiments; OBT, WH, JS, XHY and IPM participated in data analysis. IPM directed the project; OBT and IPM drafted the manuscript. All authors contributed to the final manuscript.

Acknowledgements

We acknowledge the assistance of Lorenzo Pesce for using the super computer BEAGLE under grant 1S10OD018495-01.

Conflict of Interest statement. None declared.

Funding

This work was supported by National Institutes of Health (R01 HL092153 and R01 HL124836 to I.P.M., T32 GM007183 and HL007381 to J.D.S.) and American Heart Association (13POST17290028 to O.B.T.).

References

1. Gelb, B.D. and Chung, W.K. (2014) Complex genetics and the etiology of human congenital heart disease. *Cold Spring Harb. Perspect. Med.*, **4**, a013953.
2. Srivastava, D. (2006) Making or breaking the heart: from lineage determination to morphogenesis. *Cell*, **126**, 1037–1048.
3. Hoffman, J.I. and Kaplan, S. (2002) The incidence of congenital heart disease. *J. Am. Coll. Cardiol.*, **39**, 1890–2000.
4. Pierpont, M.E., Markwald, R.R. and Lin, A.E. (2000) Genetic aspects of atrioventricular septal defects. *Am. J. Med. Genet.*, **97**, 289–296.
5. Burn, J., Brennan, P., Little, J., Holloway, S., Coffey, R., Somerville, J., Dennis, N.R., Allan, L., Arnold, R., Deanfield, J.E. *et al.* (1998) Recurrence risks in offspring of adults with major heart defects: results from first cohort of British collaborative study. *Lancet*, **351**, 311–316.
6. Calcagni, G., Digilio, M.C., Sarkozy, A., Dallapiccola, B. and Marino, B. (2007) Familial recurrence of congenital heart disease: an overview and review of the literature. *Eur. J. Pediatr.*, **166**, 111–116.
7. Gill, H.K., Splitt, M., Sharland, G.K. and Simpson, J.M. (2003) Patterns of recurrence of congenital heart disease: an analysis of 6,640 consecutive pregnancies evaluated by detailed fetal echocardiography. *J. Am. Coll. Cardiol.*, **42**, 923–929.
8. Kamp, A., Peterson, M.A., Svenson, K.L., Bjork, B.C., Hentges, K.E., Rajapaksha, T.W., Moran, J., Justice, M.J., Seidman, J.G., Seidman, C.E. *et al.* (2010) Genome-wide identification of mouse congenital heart disease loci. *Hum. Mol. Genet.*, **19**, 3105–31013.
9. Kelly, R.G., Brown, N.A. and Buckingham, M.E. (2001) The arterial pole of the mouse heart forms from Fgf10-expressing cells in pharyngeal mesoderm. *Dev. Cell.*, **1**, 435–440.
10. Waldo, K.L., Kumiski, D.H., Wallis, K.T., Stadt, H.A., Hutson, M.R., Platt, D.H. and Kirby, M.L. (2001) Conotruncal myocardium arises from a secondary heart field. *Development*, **128**, 3179–3188.
11. Xie, L., Hoffmann, A.D., Burnicka-Turek, O., Friedland-Little, J.M., Zhang, K. and Moskowitz, I.P. (2012) Tbx5-hedgehog molecular networks are essential in the second heart field for atrial septation. *Dev. Cell.*, **23**, 280–291.
12. Hoffmann, A.D., Peterson, M.A., Friedland-Little, J.M., Anderson, S.A. and Moskowitz, I.P. (2009) Sonic hedgehog is required in pulmonary endoderm for atrial septation. *Development*, **136**, 1761–1770.
13. Goddeeris, M.M., Rho, S., Petiet, A., Davenport, C.L., Johnson, G.A., Meyers, E.N. and Klingensmith, J. (2008) Intracardiac septation requires hedgehog-dependent cellular contributions from outside the heart. *Development*, **135**, 1887–1895.
14. Snarr, B.S., Wirrig, E.E., Phelps, A.L., Trusk, T.C. and Wessels, A. (2007) A spatiotemporal evaluation of the contribution of the dorsal mesenchymal protrusion to cardiac development. *Dev. Dyn.*, **236**, 1287–1294.
15. Mommersteeg, M.T., Soufan, A.T., de Lange, F.J., van den Hoff, M.J., Anderson, R.H., Christoffels, V.M. and Moorman, A.F. (2006) Two distinct pools of mesenchyme contribute to the development of the atrial septum. *Circ. Res.*, **99**, 351–353.
16. Blom, N.A., Ottenka, J., Wenink, A.G. and Gittenberger-de Groot, A.C. (2003) Deficiency of the vestibular spine in atrioventricular septal defects in human fetuses with Down syndrome. *Am. J. Cardiol.*, **91**, 180–184.
17. Briggs, L.E., Kakarla, J. and Wessels, A. (2012) The pathogenesis of atrial and atrioventricular septal defects with special emphasis on the role of the dorsal mesenchymal protrusion. *Differentiation*, **84**, 117–130.
18. Friedland-Little, J.M., Hoffmann, A.D., Ocbina, P.J., Peterson, M.A., Bosman, J.D., Chen, Y., Cheng, S.Y., Anderson, K.V. and Moskowitz, I.P. (2011) A novel murine allele of Intraflagellar Transport Protein 172 causes a syndrome including VACTERL-like features with hydrocephalus. *Hum. Mol. Genet.*, **20**, 3725–3737.
19. Huangfu, D., Liu, A., Rakeman, A.S., Murcia, N.S., Niswander, L. and Anderson, K.V. (2003) Hedgehog signaling in the mouse requires intraflagellar transport proteins. *Nature*, **426**, 83–87.
20. Francou, A., Saint-Michel, E., Mesbah, K. and Kelly, R.G. (2014) TBX1 regulates epithelial polarity and dynamic basal filopodia in the second heart field. *Development*, **141**, 4320–4331.
21. Maslen, C.L., Babcock, D., Robinson, S.W., Bean, L.J., Dooley, K.J., Willour, V.L. and Sherman, S.L. (2006) CRELD1 mutations contribute to the occurrence of cardiac atrioventricular septal defects in Down syndrome. *Am. J. Med. Genet.*, **140**, 2501–2505.

22. Blacque, O.E., Perens, E.A., Boroevich, K.A., Inglis, P.N., Li, C., Warner, A., Khattra, J., Holt, R.A., Ou, G., Mah, A.K. *et al.* (2005) Functional genomics of the cilium, a sensory organelle. *Curr. Biol.*, **15**, 935–941.
23. Kennedy, M.P., Omran, H., Leigh, M.W., Dell, S., Morgan, L., Molina, P.L., Robinson, B.V., Minnix, S.L., Olbrich, H., Severin, T. *et al.* (2007) Congenital heart disease and other heterotaxic defects in a large cohort of patients with primary ciliary dyskinesia. *Circulation*, **115**, 2814–2821.
24. Francis, R.J., Christopher, A., Devine, W.A., Ostrowski, L. and Lo, C. (2012) Congenital heart disease and the specification of left-right asymmetry. *Am. J. Physiol. Heart Circ. Physiol.*, **302**, H2102–H2111.
25. Tan, S.Y., Rosenthal, J., Zhao, X.Q., Francis, R.J., Chatterjee, B., Sabol, S.L., Linask, K.L., Bracero, L., Connelly, P.S., Daniels, M.P. *et al.* (2007) Heterotaxy and complex structural heart defects in a mutant mouse model of primary ciliary dyskinesia. *J. Clin. Invest*, **117**, 3742–3752.
26. Kathiriya, I.S. and Srivastava, D. (2000) Left-right asymmetry and cardiac looping: implications for cardiac development and congenital heart disease. *Am. J. Med. Genet.*, **97**, 271–279.
27. Seo, J.W., Brown, N.A., Ho, S.Y. and Anderson, R.H. (1992) Abnormal laterality and congenital cardiac anomalies. Relations of visceral and cardiac morphologies in the iv/iv mouse. *Circulation*, **86**, 642–650.
28. Icardo, J.M. and Sanchez de Vega, M.J. (1991) Spectrum of heart malformations in mice with situs solitus, situs inversus, and associated visceral heterotaxy. *Circulation*, **84**, 2547–2558.
29. Cui, C., Chatterjee, B., Francis, D., Yu, Q., SanAgustin, J.T., Francis, R., Tansey, T., Henry, C., Wang, B., Lemley, B. *et al.* (2011) Disruption of Mks1 localization to the mother centriole causes cilia defects and developmental malformations in Meckel-Gruber syndrome. *Dis. Model. Mech.*, **4**, 43–56.
30. Tammachote, R., Hommerding, C.J., Sinders, R.M., Miller, C.A., Czarnecki, P.G., Leightner, A.C., Salisbury, J.L., Ward, C.J., Torres, V.E., Gattone, V.H. *et al.* (2009) Ciliary and centrosomal defects associated with mutation and depletion of the Meckel syndrome genes MKS1 and MKS3. *Hum. Molec. Genet.*, **18**, 3311–3323.
31. Weatherbee, S.D., Niswander, L.A. and Anderson, K.V. (2009) A mouse model for Meckel syndrome reveals Mks1 is required for ciliogenesis and hedgehog signaling. *Hum. Molec. Genet.*, **18**, 4565–4575.
32. Dawe, H.R., Smith, U.M., Cullinane, A.R., Gerrelli, D., Cox, P., Badano, J.L., Blair-Reid, S., Sriram, N., Katsanis, N., Attie-Bitach, T. *et al.* (2007) The Meckel-Gruber Syndrome proteins MKS1 and meckelin interact and are required for primary cilium formation. *Hum. Mol. Genet*, **16**, 173–186.
33. Kyttälä, M., Tallila, J., Salonen, R., Kopra, O., Kohlschmidt, N., Paavola-Sakki, P., Peltonen, L. and Kestilä, M. (2006) MKS1, encoding a component of the flagellar apparatus basal body proteome, is mutated in Meckel syndrome. *Nat. Genet.*, **38**, 155–157.
34. Cohen, M., Kicheva, A., Ribeiro, A., Blassberg, R., Page, K.M., Barnes, C.P. and Briscoe, J. (2015) Ptch1 and Gli regulate Shh signalling dynamics via multiple mechanisms. *Nat. Commun.*, **6**, 6709.
35. Grachtchouk, V., Grachtchouk, M., Lowe, L., Johnson, T., Wei, L., Wang, A., de Sauvage, F. and Dlugosz, A.A. (2003) The magnitude of hedgehog signaling activity defines skin tumor phenotype. *Embo J.*, **22**, 2741–2751.
36. Knowles, M.R., Leigh, M.W., Carson, J.L., Davis, S.D., Dell, S.D., Ferkol, T.W., Olivier, K.N., Sagel, S.D., Rosenfeld, M., Burns, K.A. *et al.* (2012) Mutations of DNAH11 in patients with primary ciliary dyskinesia with normal ciliary ultrastructure. *Thorax*, **67**, 433–4341.
37. Lucas, J.S., Adam, E.C., Goggin, P.M., Jackson, C.L., Powles-Glover, N., Patel, S.H., Humphreys, J., Fray, M.D., Falconnet, E., Blouin, J.L. *et al.* (2012) Static respiratory cilia associated with mutations in Dnahc11/DNAH11: a mouse model of PCD. *Hum. Mutat.*, **33**, 495–503.
38. Chapelin, C., Duriez, B., Magnino, F., Goossens, M., Escudier, E. and Amselem, S. (1997) Isolation of several human axonemal dynein heavy chain genes: genomic structure of the catalytic site, phylogenetic analysis and chromosomal assignment. *FEBS Lett.*, **412**, 325–330.
39. Supp, D.M., Brueckner, M., Kuehn, M.R., Witte, D.P., Lowe, L.A., McGrath, J., Corrales, J. and Potter, S.S. (1999) Targeted deletion of the ATP binding domain of left-right dynein confirms its role in specifying development of left-right asymmetries. *Development*, **26**, 5495–5404.
40. Supp, D.M., Witte, D.P., Potter, S.S. and Brueckner, M. (1997) Mutation of an axonemal dynein affects left-right asymmetry in inversus viscerum mice. *Nature*, **389**, 963–966.
41. Pifferi, M., Michelucci, A., Conidi, M.E., Cangiotti, A.M., Simi, P., Macchia, P. and Boner, A.L. (2010) New DNAH11 mutations in primary ciliary dyskinesia with normal axonemal ultrastructure. *Eur. Respir. J.*, **35**, 1413–1416.
42. Escudier, E., Duquesnoy, P., Papon, J.F. and Amselem, S. (2009) Ciliary defects and genetics of primary ciliary dyskinesia. *Paediatr. Respir. Rev.*, **10**, 51–54.
43. Schwabe, G.C., Hoffmann, K., Loges, N.T., Birker, D., Rossier, C., de Santi, M.M., Olbrich, H., Fliegauf, M., Failly, M., Liebers, U. *et al.* (2008) Primary ciliary dyskinesia associated with normal axoneme ultrastructure is caused by DNAH11 mutations. *Hum. Mutat.*, **29**, 289–298.
44. Bartoloni, L., Blouin, J.L., Pan, Y., Gehrig, C., Maiti, A.K., Scamuffa, N., Rossier, C., Jorissen, M., Armengot, M., Meeks, M. *et al.* (2002) Mutations in the DNAH11 (axonemal heavy chain dynein type 11) gene cause one form of situs inversus totalis and most likely primary ciliary dyskinesia. *Proc. Natl. Acad. Sci USA*, **99**, 10282–10286.
45. Ermakov, A., Stevens, J.L., Whitehill, E., Robson, J.E., Pieles, G., Brooker, D., Goggolidou, P., Powles-Glover, N., Hacker, T., Young, S.R. *et al.* (2009) Mouse mutagenesis identifies novel roles for left-right patterning genes in pulmonary, craniofacial, ocular, and limb development. *Dev. Dyn.*, **238**, 581–594.
46. Consugar, M.B., Kubly, V.J., Lager, D.J., Hommerding, C.J., Wong, W.C., Bakker, E., Gattone, V.H., Torres, V.E., Breuning, M.H. and Harris, P.C. (2007) Molecular diagnostics of Meckel-Gruber syndrome highlights phenotypic differences between MKS1 and MKS3. *Hum. Genet.*, **121**, 591–599.
47. Leitch, C.C., Zaghloul, N.A., Davis, E.E., Stoetzel, C., Diaz-Font, A., Rix, S., Alfadhel, M., Lewis, R.A., Eyaid, W., Banin, E. *et al.* (2008) Hypomorphic mutations in syndromic encephalocele genes are associated with Bardet-Biedl syndrome. *Nat. Genet.*, **40**, 443–448.
48. Auber, B., Burfeind, P., Herold, S., Schoner, K., Simson, G., Rauskolb, R. and Rehder, H. (2007) A disease causing deletion of 29 base pairs in intron 15 in the MKS1 gene is highly associated with the campomelic variant of the Meckel-Gruber syndrome. *Clin. Genet.*, **72**, 454–459.
49. Hoffmann, A.D., Yang, X.H., Burnicka-Turek, O., Bosman, J.D., Ren, X., Steimle, J.D., Vokes, S.A., McMahon, A.P.,

Kalinichenko, V.V. and Moskowitz, I.P. (2014) Foxf genes integrate Tbx5 and Hedgehog pathways in the second heart field for cardiac septation. *PLOS Genet.*, **10**, e1004604.
50. Medina-Martínez, O. and Ramírez-Solis, R. (2003) In vivo mutagenesis of the Hoxb8 hexapeptide domain leads to dominant homeotic transformations that mimic the loss-of-function mutations in genes of the Hoxb cluster. *Dev. Biol.*, **264**, 77–90.
51. Inglis, P.N., Boroevich, K.A. and Leroux, M.R. (2006) Piecing together a ciliome. *Trends Genet.*, **22**, 491–500.
52. Davis, E.E. and Katsanis, N. (2012) The ciliopathies: a transitional model into systems biology of human genetic disease. *Curr. Opin. Genet. Dev.*, **22**, 290–303.
53. Garcia-Gonzalo, F.R., Corbit, K.C., Sirerol-Piquer, M.S., Ramaswami, G., Otto, E.A., Noriega, T.R., Seol, A.D., Robinson, J.F., Bennett, C.L., Josifova, D.J. *et al.* (2011) A Transition Zone Complex Regulates Mammalian Ciliogenesis and Ciliary Membrane Composition. *Nat. Genet.*, **43**, 776–784.
54. Gerdes, J.M., Davis, E.E. and Katsanis, N. (2009) The vertebrate primary cilium in development, homeostasis, and disease. *Cell*, **137**, 32–45.
55. Baker, K. and Beales, P.L. (2009) Making sense of cilia in disease: the human ciliopathies. *Am. J. Med. Genet. C. Semin. Med. Genet.*, **151C**, 281–295.
56. Badano, J.L., Mitsuma, N., Beales, P.L. and Katsanis, N. (2006) The ciliopathies: an emerging class of human genetic disorders. *Annu. Rev. Genomics. Hum. Genet*, **7**, 125–148.
57. Koefoed, K., Veland, I.R., Pedersen, L.B., Larsen, L.A. and Christensen, S.T. (2004) Cilia and coordination of signaling networks during heart development. *Organogenesis*, **10**, 108–125.
58. Karp, N., Grosse-Wortmann, L. and Bowdin, S. (2012) Severe aortic stenosis, bicuspid aortic valve and atrial septal defect in a child with Joubert Syndrome and Related Disorders (JSRD) - a case report and review of congenital heart defects reported in the human ciliopathies. *Eur. J. Med. Genet.*, **55**, 605–610.
59. Zariwala, M.A., Knowles, M.R., Leigh, M.W. (2007). Primary Ciliary Dyskinesia. In: Pagon RA, Adam MP, Ardinger HH. *et al.* editors. GeneReviews® [Internet]. Seattle (WA): University of Washington, Seattle; 1993-2014. Available from: http://www.ncbi.nlm.nih.gov/books/NBK1122/
60. Liu, C., Liu, W., Palie, J., Lu, M.F., Brown, N.A. and Martin, J.F. (2002) Pitx2c patterns anterior myocardium and aortic arch vessels and is required for local cell movement into atrioventricular cushions. *Development*, **129**, 5081–5091.
61. Li, Z.J., Nieuwenhuis, E., Nien, W., Zhang, X., Zhang, J., Puviindran, V., Wainwright, B.J., Kim, P.C. and Hui, C.C. (2012) Kif7 regulates Gli2 through Sufu-dependent and -independent functions during skin development and tumorigenesis. *Development*, **139**, 4152–4161.
62. Lo, C. (2011). Information submitted by the NHLBI Cardiovascular Development Consortium (CvDC), Bench to Bassinet Program MGI Direct Data Submission (B2B/CvDC) [MGI Ref ID J:175213].
63. Modeling the Genetic Basis for Human Congenital Heart Disease in Mice http://www.devbio.pitt.edu/research/mouse_muta.html
64. Liem, K.F., He, M., Ocbina, P.J. and Anderson, K.V. (2009) Mouse Kif7/Costal2 is a cilia-associated protein that regulates Sonic hedgehog signaling. *Proc. Natl. Acad. Sci. USA*, **106**, 13377–13382.
65. Heydeck, W., Zeng, H. and Liu, A. (2009) Planar cell polarity effector gene Fuzzy regulates cilia formation and Hedgehog signal transduction in mouse. *Dev. Dyn.*, **238**, 3035–3042.
66. Svärd, J., Heby-Henricson, K., Persson-Lek, M., Rozell, B., Lauth, M., Bergström, A., Ericson, J., Toftgård, R. and Teglund, S. (2006) Genetic elimination of Suppressor of fused reveals an essential repressor function in the mammalian Hedgehog signaling pathway. *Dev. Cell.*, **10**, 187–197.
67. Chen, C.P. (2007) Meckel syndrome: genetics, perinatal findings, and differential diagnosis. *Taiwan J. Obstet. Gynecol.*, **46**, 9–14.
68. Katsanis, N., Ansley, S.J., Badano, J.L., Eichers, E.R., Lewis, R.A., Hoskins, B.E., Scambler, P.J., Davidson, W.S., Beales, P.L. and Lupski, J.R. (2001) Triallelic inheritance in Bardet-Biedl syndrome, a mendelian recessive disorder. *Science*, **293**, 2256–2259.
69. Salonen, R. and Paavola, P. (1998) Meckel syndrome. *J. Med. Genet.*, **35**, 497–501.
70. Sepulveda, W., Sebire, N.J., Souka, A., Snijders, R.J. and Nicolaides, K.H. (1997) Diagnosis of the Meckel-Gruber syndrome at eleven to fourteen weeks' gestation. *Am. J. Obstet. Gynecol.*, **176**, 316–319.
71. Nyberg, D.A., Hallesy, D., Mahony, B.S., Hirsch, J.H., Luthy, D.A. and Hickok, D. (1990) Meckel-Gruber syndrome. Importance of prenatal diagnosis. *J. Ultrasound. Med.*, **9**, 691–696.
72. Salonen, R. (1984) The Meckel syndrome: clinicopathological findings in 67 patients. *Am. J. Med. Genet.*, **18**, 671–689.
73. Fraser, F.C. and Lytwyn, A. (1981) Spectrum of anomalies in the Meckel syndrome, or: "Maybe there is a malformation syndrome with at least one constant anomaly". *Am. J. Med. Genet.*, **9**, 67–73.
74. Rupp, P.A., Fouad, G.T., Egelston, C.A., Reifsteck, C.A., Olson, S.B., Knosp, W.M., Glanville, R.W., Thornburg, K.L., Robinson, S.W. and Maslen, C.L. (2002) Identification, genomic organization and mRNA expression of CRELD1, the founding member of a unique family of matricellular proteins. *Gene*, **293**, 47–57.
75. Redig, J.K., Fouad, G.T., Babcock, D., Reshey, B., Feingold, E., Reeves, R.H. and Maslen, C.L. (2014) Allelic Interaction between CRELD1 and VEGFA in the Pathogenesis of Cardiac Atrioventricular Septal Defects. *AIMS Genet.*, **1**, 1–19.
76. Fairfield, H., Gilbert, G.J., Barter, M., Corrigan, R.R., Curtain, M., Ding, Y., D'Ascenzo, M., Gerhardt, D.J., He, C., Huang, W. *et al.* (2011) Mutation discovery in mice by whole exome sequencing. *Genome Biol.*, **12**, R86.
77. Buchovecky, C.M., Turley, S.D., Brown, H.M., Kyle, S.M., McDonald, J.G., Liu, B., Pieper, A.A., Huang, W., Katz, D.M., Russell, D.W. *et al.* (2013) A suppressor screen in Mecp2 mutant mice implicates cholesterol metabolism in Rett syndrome. *Nat. Genet.*, **45**, 1013–1020.
78. Li, H. and Durbin, R. (2010) Fast and accurate long-read alignment with Burrows-Wheeler Transform. *Bioinformatics*, **26**, 589–595.
79. Li, H., Handsaker, B., Wysoker, A., Fennell, T., Ruan, J., Homer, N., Marth, G., Abecasis, G. and Durbin, R. (2009) The Sequence Alignment/Map format and SAMtools. *Bioinformatics*, **25**, 2078–2079.
80. Choi, Y., Sims, G.E., Murphy, S., Miller, J.R. and Chan, A.P. (2012) Predicting the functional effect of amino acid substitutions and indels. *PLoS One*, **7**, e46688.
81. Sievers, F., Wilm, A., Dineen, D., Gibson, T.J., Karplus, K., Li, W., Lopez, R., McWilliam, H., Remmert, M., Söding, J. *et al.* (2011) Fast, scalable generation of high-quality protein multiple sequence alignments using Clustal Omega. *Mol. Syst. Biol.*, **7**, 539.
82. Adzhubei, I.A., Schmidt, S., Peshkin, L., Ramensky, V.E., Gerasimova, A., Bork, P., Kondrashov, A.S. and Sunyaev,

S.R. (2010) A method and server for predicting damaging missense mutations. *Nat. Methods.*, **7**, 248–249.
83. Livak, K.J. and Schmittgen, T.D. (2001) Analysis of relative gene expression data using real-time quantitative PCR and the 2(-Delta Delta C(T)) method. *Methods*, **25**, 402–408.
84. Moorman, A.F., Houweling, A.C., de Boer, P.A. and Christoffels, V.M. (2001) Sensitive nonradioactive detection of mRNA in tissue sections: novel application of the whole-mount in situ hybridization protocol. *J Histochem Cytochem.*, **49**, 1–8.
85. Kim, D., Pertea, G., Trapnell, C., Pimentel, H., Kelley, R. and Salzberg, S.L. (2013) TopHat2: accurate alignment of transcriptomes in the presence of insertions, deletions and gene fusions. *Genome Biol.*, **14**, R36.
86. Liao, Y., Smyth, G.K. and Shi, W. (2014) FeatureCounts: an efficient general purpose program for assigning sequence reads to genomic features. *Bioinformatics*, **30**, 923–930.
87. Love, M.I., Huber, W. and Anders, S. (2014) Moderated estimation of fold change and dispersion for RNA-seq data with DESeq2. *Genome Biol.*, **15**, 550.
88. Li, Y., Klena, N.T., Gabriel, G.C., Liu, X., Kim, A.J., Lemke, K., Chen, Y., Chatterjee, B., Devine, W., Damerla, R.R. *et al.* (2015) Global genetic analysis in mice unveils central role for cilia in congenital heart disease. *Nature*, **521**, 520–524.
89. Damerla, R.R., Chatterjee, B., Li, Y., Francis, R.J., Fatakia, S.N. and Lo, C.W. (2014) Ion Torrent sequencing for conducting genome-wide scans for mutation mapping analysis. *Mamm. Genome*, **25**, 120–128.
90. Nakhleh, N., Francis, R., Giese, R.A., Tian, X., Li, Y., Zariwala, M.A., Yagi, H., Khalifa, O., Kureshi, S., Chatterjee, B. *et al.* (2012) High prevalence of respiratory ciliary dysfunction in congenital heart disease patients with heterotaxy. *Circulation*, **125**, 2232–2242.
91. Zariwala, M.A., Omran, H. and Ferkol, T.W. (2011) The Emerging Genetics of Primary Ciliary Dyskinesia. *Proc. Am. Thorac. Soc.*, **8**, 430–433.
92. Leigh, M.W., Zariwala, M.A. and Knowles, M.R. (2009) Primary ciliary dyskinesia: improving the diagnostic approach. *Curr. Opin. Pediatr.*, **21**, 320–325.
93. Zariwala, M.A., Knowles, M.R. and Omran, H. (2007) Genetic defects in ciliary structure and function. *Annu. Rev. Physiol.*, **69**, 423–450.
94. Ostrowski, L.E., Yin, W., Rogers, T.D., Busalacchi, K.B., Chua, M., O'Neal, W.K. and Grubb, B.R. (2010) Conditional deletion of Dnaic1 in a murine model of primary ciliary dyskinesia causes chronic rhinosinusitis. *Am. J. Respir. Cell Mol. Biol.*, **43**, 56–63.
95. Brueckner, M. (2007) Heterotaxia, congenital heart disease, and primary ciliary dyskinesia. *Circulation*, **115**, 2793–2795.
96. van's Gravesande, K.S. and Omran, H. (2005) Primary ciliary dyskinesia: clinical presentation, diagnosis and genetics. *Ann. Med.*, **37**, 439–449.
97. El Zein, L., Omran, H. and Bouvagnet, P. (2003) Lateralization defects and ciliary dyskinesia: lessons from algae. *Trends Genet.*, **19**, 162–167.
98. Skarnes, W.C., Rosen, B., West, A.P., Koutsourakis, M., Bushell, W., Iyer, V., Mujica, A.O., Thomas, M., Harrow, J., Cox, T. *et al.* (2011) A conditional knockout resource for the genome-wide study of mouse gene function. *Nature*, **474**, 337–342.
99. Ibanez-Tallon, I., Pagenstecher, A., Fliegauf, M., Olbrich, H., Kispert, A., Ketelsen, U.P., North, A., Heintz, N. and Omran, H. (2004) Dysfunction of axonemal dynein heavy chain Mdnah5 inhibits ependymal flow and reveals a novel mechanism for hydrocephalus formation. *Hum. Mol. Genet.*, **13**, 2133–2141.
100. Ibanez-Tallon, I., Gorokhova, S. and Heintz, N. (2002) Loss of function of axonemal dynein Mdnah5 causes primary ciliary dyskinesia and hydrocephalus. *Hum. Mol. Genet.*, **11**, 715–721.
101. McGrath, J., Somlo, S., Makova, S., Tian, X. and Brueckner, M. (2003) Two populations of node monocilia initiate left-right asymmetry in the mouse. *Cell*, **114**, 61–73.
102. Icardo, J.M. and Colvee, E. (2001) Origin and course of the coronary arteries in normal mice and in iv/iv mice. *J. Anat.*, **199**, 473–482.
103. Aylsworth, A.S. (2001) Clinical aspects of defects in the determination of laterality. *Am. J. Med. Genet.*, **101**, 345–355.
104. Okada, Y., Nonaka, S., Tanaka, Y., Saijoh, Y., Hamada, H. and Hirokawa, N. (1999) Abnormal nodal flow precedes situs inversus in iv and inv mice. *Mol. Cell.*, **4**, 459–468.
105. Layton, W.M. (1976) Random determination of a developmental process: reversal of normal visceral asymmetry in the mouse. *J. Hered.*, **67**, 336–338.
106. Hummel, K.P. and Chapman, D.B. (1959) Visceral inversion and associated anomalies in the mouse. *J. Hered.*, **50**, 9–13.
107. Layton, W.M., Layton, M.W., Binder, M., Kurnit, D.M., Hanzlik, A.J., Van Keuren, M. and Biddle, F.G. (1993) Expression of the IV (reversed and/or heterotaxic) phenotype in SWV mice. *Teratology*, **47**, 595–602.
108. Eguether, T., San Agustin, J.T., Keady, B.T., Jonassen, J.A., Liang, Y., Francis, R., Tobita, K., Johnson, C.A., Abdelhamed, Z.A., Lo, C.W. *et al.* (2014) IFT27 links the BBSome to IFT for maintenance of the ciliary signaling compartment. *Dev. Cell.*, **31**, 279–290.
109. Keady, B.T., Samtani, R., Tobita, K., Tsuchya, M., San Agustin, J.T., Follit, J.A., Jonassen, J.A., Subramanian, R., Lo, C.W. and Pazour, G.J. (2012) IFT25 links the signal-dependent movement of Hedgehog components to intraflagellar transport. *Dev. Cell.*, **22**, 940–951.
110. Willaredt, M.A., Gorgas, K., Gardner, H.A. and Tucker, K.L. (2012) Multiple essential roles for primary cilia in heart development. *Cilia*, **1**, 23.
111. Willaredt, M.A., Hasenpusch-Theil, K., Gardner, H.A., Kitanovic, I., Hirschfeld-Warneken, V.C., Gojak, C.P., Gorgas, K., Bradford, C.L., Spatz, J., Wölfl, S. *et al.* (2008) A crucial role for primary cilia in cortical morphogenesis. *J. Neurosci.*, **28**, 12887–12900.
112. Bay, S.N. and Caspary, T. (2012) What are those cilia doing in the neural tube? *Cilia*, **1**, 19.
113. Heydeck, W. and Liu, A. (2011) PCP effector proteins inturned and fuzzy play nonredundant roles in the patterning but not convergent extension of mammalian neural tube. *Dev. Dyn.*, **240**, 1938–1948.
114. Willaredt, M.A., Hasenpusch-Theil, K., Gardner, H.A., Kitanovic, I., Hirschfeld-Warneken, V.C., Gojak, C.P., Gorgas, K., Bradford, C.L., Spatz, J., Wölfl, S. *et al.* (2009) The planar cell polarity effector Fuz is essential for targeted membrane trafficking, ciliogenesis and mouse embryonic development. *Nat. Cell. Biol.*, **11**, 1225–1232.
115. Obcina, P.J., Eggenschwiler, J.T., Moskowitz, I.P. and Anderson, K.V. (2011) Complex interactions between genes controlling trafficking in primary cilia. *Nat. Genet.*, **43**, 547–553.
116. García-García, M.J., Eggenschwiler, J.T., Caspary, T., Alcorn, H.L., Wyler, M.R., Huangfu, D., Rakeman, A.S., Lee, J.D., Feinberg, E.H., Timmer, J.R. *et al.* (2005) Analysis of mouse

embryonic patterning and morphogenesis by forward genetics. *Proc. Natl. Acad. Sci. USA*, **102**, 5913–5919.
117. Huangfu, D. and Anderson, K.V. (2005) Cilia and Hedgehog responsiveness in the mouse. *Proc. Natl. Acad. Sci. USA*, **102**, 11325–11330.
118. Gerdin, A.K. and White, J. (2010) The Sanger Mouse Genetics Programme: High throughput characterization of knockout mice. *Acta Ophthalmol.*, **88**, 925–927.
119. Katsanis, N. (2006) Ciliary proteins and exencephaly. *Nat. Genet.*, **38**, 135–136.
120. Braithwaite, J.M. and Economides, D.L. (1995) First-trimester diagnosis of Meckel-Gruber syndrome by transabdominal sonography in a low-risk case. *Prenat. Diagn.*, **15**, 1168–1170.
121. Mecke, S. and Passarge, E. (1971) Encephalocele, polycystic kidneys, and polydactyly as an autosomal recessive trait simulating certain other disorders: the Meckel syndrome. *Ann. Genet*, **14**, 97–103.
122. Wheway, G., Abdelhamed, Z., Natarajan, S., Toomes, C., Inglehearn, C. and Johnson, C.A. (2013) Aberrant Wnt signalling and cellular over-proliferation in a novel mouse model of Meckel–Gruber syndrome. *Dev. Biol.*, **377**, 55–66.
123. White, J.K., Gerdin, A.K., Karp, N.A., Ryder, E., Buljan, M., Bussell, J.N., Salisbury, J., Clare, S., Ingham, N.J., Podrini, C. *et al.* (2013) Genome-wide generation and systematic phenotyping of knockout mice reveals new roles for many genes. *Cell*, **154**, 452–464.
124. Wellcome Trust Sanger Institute. (2010) Alleles produced for the EUCOMM and EUCOMMTools projects by the Wellcome Trust Sanger Institute. MGI Direct Data Submission, J:155845.
125. Dowdle, W.E., Robinson, J.F., Kneist, A., Sirerol-Piquer, M.S., Frints, S.G., Corbit, K.C., Zaghloul, N.A., van Lijnschoten, G., Mulders, L., Verver, D.E. *et al.* (2011) Disruption of a ciliary B9 protein complex causes Meckel syndrome. *Am. J. Hum. Genet.*, **89**, 94–110.
126. Chih, B., Liu, P., Chinn, Y., Chalouni, C., Komuves, L.G., Hass, P.E., Sandoval, W. and Peterson, A.S. (2011) A ciliopathy complex at the transition zone protects the cilia as a privileged membrane domain. *Nat. Cell. Biol.*, **14**, 61–72.
127. Bergmann, C., Fliegauf, M., Brüchle, N.O., Frank, V., Olbrich, H., Kirschner, J., Schermer, B., Schmedding, I., Kispert, A., Kränzlin, B. *et al.* (2008) Loss of nephrocystin-3 function can cause embryonic lethality, Meckel-Gruber-like syndrome, situs inversus, and renal-hepatic-pancreatic dysplasia. *Am. J. Hum. Genet.*, **82**, 959–970.
128. Ko, H.W., Norman, R.X., Tran, J., Fuller, K.P., Fukuda, M. and Eggenschwiler, J.T. (2010) Broad-minded links cell cycle-related kinase to cilia assembly and hedgehog signal transduction. *Dev. Cell.*, **18**, 237–247.
129. Ezratty, E.J., Stokes, N., Chai, S., Shah, A.S., Williams, S.E. and Fuchs, E. (2011) A role for the primary cilium in Notch signaling and epidermal differentiation during skin development. *Cell*, **145**, 1129–1141.
130. Bell, S.E., Mavila, A., Salazar, R., Bayless, K.J., Kanagala, S., Maxwell, S.A. and Davis, G.E. (2001) Differential gene expression during capillary morphogenesis in 3D collagen matrices: regulated expression of genes involved in basement membrane matrix assembly, cell cycle progression, cellular differentiation and G-protein signaling. *J. Cell. Sci.*, **114**, 2755–2773.
131. Tong, C.K., Han, Y.G., Shah, J.K., Obernier, K., Guinto, C.D. and Alvarez-Buylla, A. (2014) Primary cilia are required in a unique subpopulation of neural progenitors. *Proc. Natl. Acad. Sci. USA*, **111**, 12438–12443.
132. Zhang, Q., Seo, S., Bugge, K., Stone, E.M. and Sheffield, V.C. (2012) BBS proteins interact genetically with the IFT pathway to influence SHH-related phenotypes. *Hum. Mol. Genet.*, **21**, 1945–1953.
133. McIntyre, J.C., Davis, E.E., Joiner, A., Williams, C.L., Tsai, I.C., Jenkins, P.M., McEwen, D.P., Zhang, L., Escobado, J., Thomas, S. *et al.* (2012) Gene therapy rescues cilia defects and restores olfactory function in a mammalian ciliopathy model. *Nat. Med.*, **18**, 1423–1428.
134. Clement, C.J., Kristensen, S.G., Møllgård, K., Pazour, G.J., Yoder, B.K., Larsen, L.A. and Christensen, S.T. (2009) The primary cilium coordinates early cardiogenesis and hedgehog signaling in cardiomyocyte differentiation. *J. Cell. Sci.*, **122**, 3070–3082.
135. Lehman, J.M., Michaud, E.J., Schoeb, T.R., Aydin-Son, Y., Miller, M. and Yoder, B.K. (2008) The Oak Ridge Polycystic Kidney mouse: modeling ciliopathies of mice and men. *Dev. Dyn.*, **237**, 1960–1971.
136. Slough, J., Cooney, L. and Brueckner, M. (2008) Monocilia in the embryonic mouse heart suggest a direct role for cilia in cardiac morphogenesis. *Dev. Dyn.*, **237**, 2304–2314.
137. Haycraft, C.J., Zhang, Q., Song, B., Jackson, W.S., Detloff, P.J., Serra, R. and Yoder, B.K. (2007) Intraflagellar transport is essential for endochondral bone formation. *Development*, **134**, 307–316.
138. Liu, A., Wang, B. and Niswander, L.A. (2005) Mouse intraflagellar transport proteins regulate both the activator and repressor functions of Gli transcription factors. *Development*, **132**, 3103–3111.
139. Taulman, P.D., Haycraft, C.J., Balkovetz, D.F. and Yoder, B.K. (2001) Polaris, a protein involved in left-right axis patterning, localizes to basal bodies and cilia. *Mol. Biol. Cell.*, **12**, 589–599.
140. Pazour, G.J., Dickert, B.L., Vucica, Y., Seeley, E.S., Rosenbaum, J.L., Witman, G.B. and Cole, D.G. (2000) Chlamydomonas IFT88 and its mouse homologue, polycystic kidney disease gene tg737, are required for assembly of cilia and flagella. *J. Cell. Biol.*, **151**, 709–718.
141. Murcia, N.S., Richards, W.G., Yoder, B.K., Mucenski, M.L., Dunlap, J.R. and Woychik, R.P. (2000) The Oak Ridge Polycystic Kidney (orpk) disease gene is required for left-right axis determination. *Development*, **127**, 2347–2355.
142. Moyer, J.H., Lee-Tischler, M.J., Kwon, H.Y., Schrick, J.J., Avner, E.D., Sweeney, W.E., Godfrey, V.L., Cacheiro, N.L., Wilkinson, J.E. and Woychik, R.P. (1994) Candidate gene associated with a mutation causing recessive polycystic kidney disease in mice. *Science*, **264**, 1329–1333.
143. Pennekamp, P., Menchen, T., Dworniczak, B. and Hamada, H. (2015) Situs inversus and ciliary abnormalities: 20 years later, what is the connection? *Cilia*, **4**,
144. Guichard, C., Harricane, M.C., Lafitte, J.J., Godard, P., Zaegel, M., Tack, V., Lalau, G. and Bouvagnet, P. (2001) Axonemal dynein intermediate-chain gene (DNAI1) mutations result in situs inversus and primary ciliary dyskinesia (Kartagener syndrome). *Am. J. Hum. Genet.*, **68**, 1030–1035.
145. Zariwala, M., Noone, P.G., Sannuti, A., Minnix, S., Zhou, Z., Leigh, M.W., Hazucha, M., Carson, J.L. and Knowles, M.R. (2001) Germline mutations in an intermediate chain dynein cause primary ciliary dyskinesia. *Am. J. Respir. Cell. Mol. Biol.*, **25**, 577–583.
146. Pennarun, G., Escudier, E., Chapelin, C., Bridoux, A.M., Cacheux, V., Roger, G., Clément, A., Goossens, M., Amselem, S. and Duriez, B. (1999) Loss-of-function mutations in a human gene related to Chlamydomonas

reinhardtii dynein IC78 result in primary ciliary dyskinesia. *Am. J. Hum. Genet.*, **65**, 1508–1519.
147. Knowles, M.R., Leigh, M.W., Ostrowski, L.E., Huang, L., Carson, J.L., Hazucha, M.J., Yin, W., Berg, J.S., Davis, S.D., Dell, S.D. *et al.* (2013) Exome sequencing identifies mutations in CCDC114 as a cause of primary ciliary dyskinesia. *Am. J. Hum. Genet.*, **92**, 99–106.
148. Failly, M., Bartoloni, L., Letourneau, A., Munoz, A., Falconnet, E., Rossier, C., de Santi, M.M., Santamaria, F., Sacco, O., DeLozier-Blanchet, C.D. *et al.* (2009) Mutations in DNAH5 account for only 15% of a non-preselected cohort of patients with primary ciliary dyskinesia. *J. Med. Genet.*, **46**, 281–286.
149. Hornef, N., Olbrich, H., Horvath, J., Zariwala, M.A., Fliegauf, M., Loges, N.T., Wildhaber, J., Noone, P.G., Kennedy, M., Antonarakis, S.E. *et al.* (2006) DNAH5 mutations are a common cause of primary ciliary dyskinesia with outer dynein arm defects. *Am. J. Respir. Crit. Care. Med.*, **174**, 120–126.
150. Olbrich, H., Häffner, K., Kispert, A., Völkel, A., Volz, A., Sasmaz, G., Reinhardt, R., Hennig, S., Lehrach, H., Konietzko, N. *et al.* (2002) Mutations in DNAH5 cause primary ciliary dyskinesia and randomization of left-right asymmetry. *Nat. Genet.*, **30**, 143–144.
151. Omran, H., Häffner, K., Völkel, A., Kuehr, J., Ketelsen, U.P., Ross, U.H., Konietzko, N., Wienker, T., Brandis, M. and Hildebrandt, F. (2000) Homozygosity mapping of a gene locus for primary ciliary dyskinesia on chromosome 5p and identification of the heavy dynein chain DNAH5 as a candidate gene. *Am. J. Respir. Cell Mol. Biol.*, **23**, 696–702.
152. Khaddour, R., Smith, U., Baala, L., Martinovic, J., Clavering, D., Shaffiq, R., Ozilou, C., Cullinane, A., Kyttälä, M., Shalev, S. *et al.* (2007) Spectrum of MKS1 and MKS3 mutations in Meckel syndrome: a genotype-phenotype correlation. Mutation in brief #960. Online. *Hum. Mutat.*, **28**, 523–524.
153. Rapola, J. and Salonen, R. (1985) Visceral anomalies in the Meckel syndrome. *Teratology*, **31**, 193–201.
154. Ueda, N., Sasaki, N., Sugita, A., Gotoh, N., Yamamoto, S., Yano, T., Ochi, H., Nishimura, T., Matsuura, S. and Fukunishi, R. (1987) Encephalocele, polycystic kidneys, and polydactyly with other defects. A necropsy case of Meckel syndrome and a review of literature. *Acta. Pathol. Jpn*, **37**, 323–330.
155. Schaefer, E., Durand, M., Stoetzel, C., Doray, B., Viville, B., Hellé, S., Danse, J.M., Hamel, C., Bitoun, P., Goldenberg, A. *et al.* (2011) Molecular diagnosis reveals genetic heterogeneity for the overlapping MKKS and BBS. *Eur. J. Med. Genet.*, **54**, 157–160.
156. Karmous-Benailly, H., Martinovic, J., Gubler, M.C., Sirot, Y., Clech, L., Ozilou, C., Auge, J., Brahimi, N., Etchevers, H., Detrait, E. *et al.* (2005) Antenatal presentation of Bardet-Biedl syndrome may mimic Meckel syndrome. *Am. J. Hum. Genet.*, **76**, 493–504.
157. Moore, S.J., Green, J.S., Fan, Y., Bhogal, A.K., Dicks, E., Fernandez, B.A., Stefanelli, M., Murphy, C., Cramer, B.CDean, J.C. *et al.* (2005) Clinical and genetic epidemiology of Bardet-Biedl syndrome in Newfoundland: a 22-year prospective, population-based, cohort study. *Am. J. Med. Genet.*, **132A**, 352–360.
158. Kim, J.C., Ou, Y.Y., Badano, J.L., Esmail, M.A., Leitch, C.C., Fiedrich, E., Beales, P.L., Archibald, J.M., Katsanis, N., Rattner, J.B. *et al.* (2005) MKKS/BBS6, a divergent chaperonin-like protein linked to the obesity disorder Bardet-Biedl syndrome, is a novel centrosomal component required for cytokinesis. *J. Cell Sci.*, **118**, 1007–1020.
159. Slavotinek, A.M., Searby, C., Al-Gazali, L., Hennekam, R.C., Schrander-Stumpel, C., Orcana-Losa, M., Pardo-Reoyo, S., Cantani, A., Kumar, D., Capellini, Q. *et al.* (2002) Mutation analysis of the MKKS gene in McKusick-Kaufman syndrome and selected Bardet-Biedl syndrome patients. *Hum. Genet.*, **110**, 561–567.
160. Slavotinek, A.M., Stone, E.M., Mykytyn, K., Heckenlively, J.R., Green, J.S., Heon, E., Musarella, M.A., Parfrey, P.S., Sheffield, V.C. and Biesecker, L.G. (2000) Mutations in MKKS cause Bardet-Biedl syndrome. *Nat. Genet.*, **26**, 15–16.
161. Slavotinek, A.M. and Biesecker, L.G. (2000) Phenotypic overlap of McKusick-Kaufman syndrome with bardet-biedl syndrome: a literature review. *Am. J. Med. Genet.*, **95**, 208–215.
162. Stone, D.L., Slavotinek, A., Bouffard, G.G., Banerjee-Basu, S., Baxevanis, A.D., Barr, M. and Biesecker, L.G. (2000) Mutation of a gene encoding a putative chaperonin causes McKusick-Kaufman syndrome. *Nat. Genet.*, **25**, 79–82.
163. David, A., Bitoun, P., Lacombe, D., Lambert, J.C., Nivelon, A., Vigneron, J. and Verloes, A. (1999) Hydrometrocolpos and polydactyly: a common neonatal presentation of Bardet-Biedl and McKusick-Kaufman syndromes. *J. Med. Genet.*, **36**, 599–603.
164. Marino, B., Ammirati, A., Borzaga, U., Giannotti, A. and Dallapiccola, B. (1999) Cardiac malformations in patients with oral-facial-skeletal syndromes: clinical similarities with heterotaxia. *Am. J. Med. Genet.*, **84**, 350–356.
165. Stone, D.L., Agarwala, R., Schäffer, A.A., Weber, J.L., Vaske, D., Oda, T., Chandrasekharappa, S.C., Francomano, C.A. and Biesecker, L.G. (1998) Genetic and physical mapping of the McKusick-Kaufman syndrome. *Hum. Mol. Genet.*, **7**, 475–481.
166. Robinow, M. and Shaw, A. (1997) The McKusick–Kaufman syndrome: recessively inherited vaginal atresia, hydrometrocolpos, uterovaginal duplications, anorectal anomalies, postaxial polydactyly, and congenital heart disease. *J. Pediatr.*, **94**, 776–778.
167. McKusick, V.A., Bauer, R.L., Koop, C.E. and Scott, R.B. (1964) Hydrometrocolpos as a simply inherited malformation. *Jama*, **189**, 813–816.
168. D'Asdia, M.C., Torrente, I., Consoli, F., Ferese, R., Magliozzi, M., Bernardini, L., Guida, V., Digilio, M.C., Marino, B., Dallapiccola, B. *et al.* (2013) Novel and recurrent EVC and EVC2 mutations in Ellis-van Creveld syndrome and Weyers acrofacial dysostosis. *Eur. J. Med. Genet.*, **56**, 80–87.
169. Hills, C.B., Kochilas, L., Schimmenti, L.A. and Moller, J.H. (2011) Ellis-van Creveld syndrome and congenital heart defects: presentation of an additional 32 cases. *Pediatr. Cardiol.*, **32**, 977–982.
170. O'Connor, M.J., Rider, N.L., Collins, R.T., Hanna, B.D., Morton, D.H. and Strauss, K.A. (2011) Contemporary management of congenital malformations of the heart in infants with Ellis - van Creveld syndrome: a report of nine cases. *Cardiol. Young*, **21**, 145–152.
171. Shen, W., Han, D., Zhang, J., Zhao, H. and Feng, H. (2011) Two novel heterozygous mutations of EVC2 cause a mild phenotype of Ellis-van Creveld syndrome in a Chinese family. *Am. J. Med. Genet.*, **155A**, 2131–2136.
172. Ruiz-Perez, V.L. and Goodship, J.A. (2009) Ellis-van Creveld syndrome and Weyers acrodental dysostosis are caused by cilia-mediated diminished response to hedgehog ligands. *Am. J. Med. Genet. C. Semin. Med. Genet.*, **151C**, 341–351.
173. Valencia, M., Lapunzina, P., Lim, D., Zannolli, R., Bartholdi, D., Wollnik, B., Al-Ajlouni, O., Eid, S.S., Cox, H., Buoni, S. *et al.* (2009) Widening the mutation spectrum of EVC and

EVC2: ectopic expression of Weyer (sic) variants in NIH 3T3 fibroblasts disrupts Hedgehog signaling. *Hum. Mutat.*, **30**, 1667–1675.
174. Sund, K.L., Roelker, S., Ramachandran, V., Durbin, L. and Benson, D.W. (2009) Analysis of Ellis van Creveld syndrome gene products: implications for cardiovascular development and disease. *Hum. Mol. Genet.*, **18**, 1813–1824.
175. Ruiz-Perez, V.L., Tompson, S.W., Blair, H.J., Espinoza-Valdez, C., Lapunzina, P., Silva, E.O., Hamel, B., Gibbs, J.L., Young, I.D., Wright, M.J. *et al.* (2003) Mutations in two non-homologous genes in a head-to-head configuration cause Ellis-van Creveld syndrome. *Am. J. Hum. Genet.*, **72**, 728–732.
176. Galdzicka, M., Patnala, S., Hirshman, M.G., Cai, J.F., Nitowsky, H., Egeland, J.A. and Ginns, E.I. (2002) A new gene, EVC2, is mutated in Ellis-van Creveld syndrome. *Mol. Genet. Metab.*, **77**, 291–295.
177. Ruiz-Perez, V.L., Ide, S.E., Strom, T.M., Lorenz, B., Wilson, D., Woods, K., King, L., Francomano, C., Freisinger, P., Spranger, S. *et al.* (2000) Mutations in a new gene in Ellis-van Creveld syndrome and Weyers acrodental dysostosis. *Nat. Genet.*, **24**, 283–286.
178. McKusick, V.A., Egeland, J.A., Eldridge, R. and Krusen, D.E. (1964) Dwarfism. In the Amish. I. The Ellis–Van Creveld Syndrome. *Bull. Johns Hopkins Hosp.*, **115**, 306–336.
179. Ellis, R.W.B. and van Creveld, S. (1940) A syndrome characterized by ectodermal dysplasia, polydactyly, chondrodysplasia and congenital morbus cordis: report of three cases. *Arch. Dis. Child.*, **15**, 65–84.